
**Università degli studi Milano-Bicocca**
Facoltà di Scienze Matematiche, Fisiche e Naturali
Dipartimento di Scienze Ambiente e Territorio e Scienze della Terra
Dottorato di Ricerca in Scienze Ambientali, XXVI Ciclo

# Computational Models To Evaluate Particulate Matter Effects on Environment and Human Health

**Marco Moscatelli**

Supervisor: Prof. Ezio Bolzacchini
External Supervisor: Dott. Alessandro Orro

Anno Accademico 2012-2013

# CONTENTS

# LIST OF FIGURES

# LIST OF TABLES

# CHAPTER 1

# INTRODUCTION

Air pollution is a problem that is becoming increasingly important in modern society as they are observed correlations between the level of pollution and damage to the environment and human health. Pollutants may be of various kinds: solid, liquid or gaseous fuels, a portion is very important and relevant to health is represented by particulate air pollution.

## 1.1 Particulate Matter

Air pollutant include any substance, natural or man-made, present in the atmosphere in sufficient concentration to have adverse effects on humans, property or the environment. The Particulate Matter (PM) is a set of particles that have physical characteristics and chemical-physical properties (size, shape,

composition, density, physical state), enabling their suspension in the atmosphere for long periods of time (hours, days or years) and which retain their characteristics for a sufficient time to enable them to participate in physical and/or chemical as entities in their own right. This definition includes a diverse set of particles, typically with very different characteristics from particle to particle, the composition of which may be different depending on the environment of origin (eg urban or rural), the time of year (summer or winter), sources (road traffic, heating, industrial or agricultural emissions, and eroded soil particles carried by the wind) and can change over time.

An important factor for the PM concentration is the Planetary Boundary Layer (PBL). In fact, if the height of the Boundary Layer increases due to the intensification of the convective motions, pollutants (both fuels, both in particulate phase) tend to be diluted in a larger volume of air and to homogenize through a high vertical mixing, making ensure that the concentrations of pollutants in soil decrease. In contrast, if its thickness is reduced, not only their dilution decreases, but in the case of thermal inversion atmospheric pollutants, released during the day, they are trapped to the ground greatly increasing the measured concentrations. The daily evolution of the PBL is shown in Figure 1.1).

This type of daily trend causes the atmospheric conditions are not always equal in time and, consequently, that they are not even the same effects of the particulates.

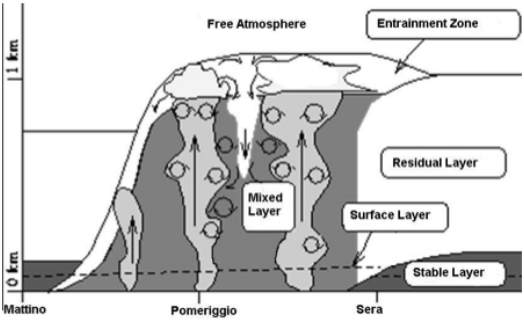


***Figure 1.1:*** *Schematic of a typical daily performance of the Planetary Boundary Layer.*

## 1.2 Computational Model

Considering the peculiarities of particulate air pollution and its relevance in the effects on human health and the environment is important to determine the concentrations and chemical compositions. For this purpose, in addition to the experimental techniques of field measurements, over the years researchers have developed various computational systems for the study of the PM from the point of view of the chemical composition of that concentration. The prediction models of PM require the implementation of different processes, including the distribution of airborne particles and their evolution in time and space.

The secondary components of PM2.5 such as NO3-, SO42-, and organic carbon (OC) are relevant in the effetcs that can be caused, so it is important implement in the model the relationships between the emissions of gaseous pollutants such

as NOx, SO2, and volatile organic compounds (VOCs) and the corresponding secondary PM2.5 constituents (Meng et al., 1997; Kumar et al., 1998; Pai et al., 2000). The implementation of these mechanisms is even more relevant when you consider that the secondary organic aerosol (SOA) comprises a large fraction of the total organic carbon aerosol (OC), often greater than 50% on a carbon mass basis (Kanakidou et al., 2005).

During the last 15-20 years different three dimensional air quality models have been developed, these model have specifics routine that consider meteorological, chemical and transport drivers.

These atmospheric chemistry-transport-dispersion models have the possibility to integrate sperimental monitoring data to calibrate the simulation and they are powerful tools to study the effects of changes of emissions, concentrations and chemical composition of particulate matter. These models used in general the same type of input data such as emissions and meteorology to calculate the concentrations of gases and aerosols.

Some meteorological drivers are:

- MM5 (PSU.NCAR, USA), (Grell et al., 1994);
- RSM (NOAA, USA), ECMWF (Redding, U.K.);
- HIRLAM (Finnish Meteorological Institute, Finland);
- WRF (Janjic et al., 2001)

Many drivers have been developed for rappresents of dispersion and chemical transport, such as:

- EUROS (RIVM, The Netherlands), (Lagner J. et al. 1998),

- EMEP Eulerian (DNMI, Oslo, Norway),
- MATCH (SMHI, Norrkoping, Sweden), (Derwent R. and Jenkin M., 1991),
- CHIMERE (ISPL, Paris, France), (Schmidt H. et al., 2001),
- DEM (NERI, Roskilde, Denmark), (Gery et al. 1989),
- STOCHEM (UK Met. Office, Bracknell, U.K.), (Collins et al., 1997) and
- CMAQ (Community Multiscale Air Quality modelling system) (Byun et al., 1998), developed by EPA (USA).
- CAMx Environ Inc., STEM-III (University of Iowa)

One of the most widely used transport models is CHIMERE, it is an off-line chemistry transport model, driven by a meteorological driver, such as MM5 or WRF. The core of CHIMERE is MELCHIOR1 (Lattuati, 1997, adapted from the original EMEP mechanism, Hov et al., 1985), which describes more than 300 reactions of 80 species. MELCHIOR1 has a high computational time therefore has been developed a reduced mechanism (MELCHIOR2) includes 44 species and about 120 reactions (Derognat et al., 2003). To calculate the equilibrium partitioning of the gas/liquid/solid aerosol in the model is included the ISORROPIA model (Nenes et al., 1998) that considered various aerosols compounds (e.g. $SO_4^{2-}$ , $NO_3$ ,$NH_4^+$ , $Na^+$, $Cl$).

As regards the determination of the meteorological variables is one of the most used models is the PSU/NCAR mesoscale model MM5 that is a limited area, non-hydrostatic or

hydrostatic designed to simulate or predict mesoscale and regional scale atmospheric circulations (Grell et al., 1994). In the last years another meteorological model has been developed, the Advanced Research WRF system that It is considered by NCAR as the successor of MM5.

The use of these models assumes, for the calculation of aerosol composition and phase state, that the system is in thermodynamic equilibrium, which is reasonable if the atmospheric processes that lead to toward equilibrium are faster compared to those that lead away from it (Wexler and Potukuchi, 1998). The phase state of atmospheric particles can be complex even when equilibrium thermodynamics applies. First, there are a wide range of possible solid phases that can form. Second, the behavior of any liquid phase in the aerosol is likely to be highly nonideal at the high solute concentrations encountered at low relative humidities. This can be a particular difficulty given that many aerosols probably exist in a metastable liquid state under some conditions, supersaturated with respect to dissolved salts (Martin, 2000). A large fraction of aerosol mass is in many cases made up of inorganic electrolyte compounds that dissociate in water to form ions and a number of models of such systems have been developed. These include:

- EQUIL (Bassett and Seinfeld, 1983)
- MARS (Saxena et al., 1986)
- EQUILIB (Pilinis and Seinfeld, 1987)
- AIM (Wexler and Seinfeld, 1991)
- SCAPE (Kim et al., 1993)

- EQUISOLV (Jacobson et al., 1996)
- ISORROPIA (Nenes et al., 1998)

Another important aspect is the ability of the particulate matter to influences the climate directly, through scattering and absorption of the solar radiation, and indirectly, through the formation of cloud condensation nuclei. The direct aerosol contribution to radiative forcing is due to sulphate aerosols, fossil fuel soot and biomass burning (Penner et al., 1993, 1994; Robock, 1991; Hansen and Lacis, 1990).

The change in aerosol chemical composition and number concentrations which subsequently alter the microphysics, radiative properties and lifetime of clouds because aerosol particles serve as cloud condensation nuclei, is referred to as the indirect radiative forcing of aerosols. This indirect effect of the aerosols can be divided into the first and second indirect effects.

In order to understand the effects of particulate air pollution on the environment and human health is important to evaluate the chemical composition of the aerosol and its distribution according to the height above the ground. With these premises we made the study: *Impact of aerosols and Black Carbon over Italian basin valleys: from high resolution measurements of vertical profiles to the modelling of radiative forcing and heating rates.* In this study we shown the first high resolution vertical profiles of aerosol radiative forcing and atmospheric heating rates based on measurements of vertical profiles of aerosols and of Black Carbon at high spatial resolution. These experimental information have been input into a model in order to compute radiative forcing and atmospheric heating rates.

Although, as we seen, a number of models have been published for the prediction of concentration and chemical composition of particulate matter, very few models have been published for predicting enviromental and human health effects. This is due that the fact the PM is a very heterogeneous class of materials, not only in terms of their chemical composition, but also in terms of size, shape, agglomeration state, and surface reactivity. So there is an urgent need to extend the knowledge to develop new methods for predicting the effects on environment and human health.

### 1.2.1 Environment Effect

The aerosol deposition due to wet or dry, can contribute to acidification (associated in particular with $H_2SO_4$ and $HNO_3$) and eutrophication (associated with nitrate salts) of the terrestrial and aquatic environments. Acidification of soils can lead to release of toxic elements such as aluminum, resulting in serious damage to the plants and various forms of aquatic life. Furthermore you have direct effects on vegetation in relation to acid and oxidizing action of the particles, which leads to damage to the plant tissues. The climate and air pollution interact to degrade the artistic, architectural and archaeological heritage.

A well-known example is the effect of disintegration of the stone materials, in particular those in calcareous component, caused by the acidity of the wet deposition (determined from atmospheric emissions of sulfur dioxide and nitrogen oxides, but also, to a lesser extent, by the presence of dissolved carbon dioxide). The erosion of the materials is mainly due to rain, sulfur depositions, nitric acid and intake of acidity. The

atmospheric particulate cause the tarnish of the materials. It was calculated that the blackening weighs 2.5 times more erosion on the dangers Atmospheric against the cultural heritage (Report on the State of the Environment in Lombardy 2001).

The corrosion may be defined as a destructive process to load the materials predominantly metal. There are basically two different corrosion processes: chemical corrosion and electrochemical corrosion. In the field of electrochemical phenomena, a special interest is played by atmospheric corrosion, since almost all of human artifacts and constantly in contact with the Earth's atmosphere, both in indoor and outdoor environments. The corrosion affecting so many fields of human activity, from the scope of construction to electronics, from the preservation of artistic and monumental in many other contexts. In the context of corrosion phenomena are therefore not considered the processes of deterioration due to mechanisms of physical type.

The corrosion thus has a strong impact on the lives and human activities. The chemical corrosion takes place in completely dry conditions, or in the total absence of moisture, therefore it is a process of secondary importance from the environmental point of view, given that in normal atmospheric conditions the total absence of moisture and an unusual situation. The electrochemical corrosion (or Galvanic) is so called because involving electrochemical redox reactions that lead to the dissolution of the metal as a result of the overall process. This type of reaction can take place either in the soil, either in the water or in moist atmospheres.

The surface of the material acts as an electrode, or as an interface between electrified a system that is located under

the electrical conduction (the material) and a second system in which the driving and of ionic type (the solution). This means that both oxidation and reduction reactions occur at the interface between the metal and the water film. The atmospheric corrosion involves different corrosive processes, mainly electrochemical type, which occur at room temperature and in which the Earth's atmosphere appears to be the corrosive environment. When it comes to atmospheric corrosion, refers to processes both outdoor and indoor.

It is a complex set of phenomena that occur at the interface between a solid phase (the material that will corrode), a thin film of water covering it (liquid state) and the atmosphere (gaseous state). These phenomena are influenced by a large number of climatic factors, such as the frequency of the rains, the humidity, the average speed of the winds, the presence of pollutants and aerosol transport phenomena. Moreover, the corrosion rate also depends on the type of metal that corrodes, from corrosion products that are formed, the possible attainment of a state of passivity, from the composition, concentration and the physico-chemical properties of the electrolytes present in the film of water.

However, the contribution of atmospheric aerosol in this process depends primarily on two factors, the first is represented by the same property of corrosivity of the aerosol, which vary in function of its chemical composition. The second important factor that determines the corrosive effects of particulate matter and the amount of aerosols that adsorbs on the film of water. It depends in turn by both the concentrations of particulates present in the atmosphere to which the material is exposed, both by the size of the particles, since they depend on

the mechanism of deposition of the particles themselves. The knowledge concerning the effects of these two factors are still relatively few, and certainly interesting to go to investigate the effects of different pollutants present in the particulate.

A rather important aspect to keep in mind when talking about the corrosive effect of the aerosol and its hygroscopicity. For hygroscopicity of a particle refers to its ability to absorb the water vapor present in the atmosphere, a phenomenon that goes to increase its size. Such property and influenced by the same diameter of the particles that make up the aerosol and by their chemical composition.

The quantity of water vapor adsorbed by a particle depends on the vapor pressure in the atmosphere and therefore the relative humidity (RH) which is located in the environment surrounding it.

The process of corrosion of a material is influenced by PM through different activities which include the presence of substances able to: change the speed of corrosion and to participate in the reactions of galvanic corrosion. Furthermore, the PM is the main responsible for the absorption of water on the metal surface.

So it is important to define the strategies for the evaluation of the effects of the particulates on the environment, particularly related to the activity of corrosion, in this context are relevant the works *Aerosol Corrosion Prevention and Energy-Saving Strategies in the Design of Green Data Centers*.

A study on the impact of the corrosivity influenced by relative humidity in indoor environments. A better knowledge of the behavior of atmospheric aerosols, with particular reference to their deliquescence crystallization, and their interac-

tions with the circuit elements of Printed Circuit Boards could allow the identification of conditions of security for data centers that optimize air conditioning systems and reduce energy consumption operated by the Data Center.

### 1.2.2 Human Health Effect

Particulate matter is characterized with major health effects that include effects on the breathing and respiratory systems, the aggravation of existing respiratory and cardiovascular diseases, the alteration of the body's defense systems against foreign materials, damage to lung tissue, carcinogenesis and premature mortality.

Various studies on air pollution effects on health have indicated a strong relationship between air pollutant concentrations and observed health effects, in particular Stern et al. (1984) and Kinami (2007) show the effect of specific air pollutants and heavy metal constituents of particulate matter on human health.

Most studies, focused on both acute and long-term effects, suggest that PM exerts significant effects on the cardiovascular system (Dockery et al., 1993; Pope et al., 1995; Samet et al., 2000), and in previous analysis (Brook et al., 2010) was shown that the major increase in mortality is associated to the cardiovascular diseases. In particular studies on animal shown a relationship between chronic PM exposure and the development of atherosclerosis(Chen and Nadziejko, 2005; Sun et al., 2005). These effects is found also in human studies where seems to be mediated by the inflammatory cytokines IL-6, TNF-$\alpha$, and C-reactive protein (CRP). Increases in both IL-6 (Ridker et al., 2000) and CRP (Wennberg et al., 2012) have been associated

with the development of acute myocardial infarction. These results are confermed in a prospective cohort study of German patients (Hoffmann et al., 2009) where is possible to link an associated exposure to PM2.5 with elevations in CRP.

Other researchers demonstrated similar increases in CRP from PM10 exposure from both combustion (Chuang et al., 2007) and organic matter (Schicker et al., 2009). On the other hand some studies have found only a weak or absent link between PM and markers of inflammation (Sullivan et al., 2007; Steinvil et al., 2008; Forbes et al., 2009; Diez-Roux et al., 2006) but these contrasts can be due to differences in composition of PM and/or exposure to differences sources of PM (Brook et al., 2010). Acute exposure to PM causes changes in coagulation and platelet activation providing a more proximal link between PM and coronary artery disease, these is probably due to the possibility of the small particles to translocate into the blood stream and exert prothrombotic effects(Nemmar et al., 2002).

Different cohort studies (Dockery et al., 1993; Pope et al., 1995, 2002, 2004; Miller et al., 2007) have shown that PM was positively associated with death from lung cancer and cardiopulmonary disease and in particular their research demonstrated an average increase in cardiopulmonary mortality of 9% for each $10\mu g/m^3$ increase in PM2.5 and increased ischemic cardiovascular disease mortality by 18% and mortality from arrhythmia, congestive heart failure, and cardiac arrest by 13%.

In addition to the effects on the cardiovascular system is important to evaluate the association between PM exposure and respiratory illness. The PM primes pulmonary oxidative stress and inflammation. Airway epithelial cells produce in-

flammatory cytokines (Silbajoris et al., 2011; Quay et al., 1998) and the alveolar macrophages react producing reactive oxygen species, nitrogen species, and release TNF-$\alpha$ and IL-1 after exposure (Driscoll et al., 1990). In mice (Riva et al., 2011) these responses have shown that can cause pulmonary damage after only a single exposure, these damages are correlated to the the primary development of asthma and chronic obstructive pulmonary disease (COPD).

Long-term exposure to PM results in airway remodeling and chronic inflammation (Hogg et al., 2004). Several controlled human experiments have demonstrated adverse affects on the pulmonary system. PM exposure has been shown to increase airway responsiveness to methacholine (Nordenhall et al., 2001), increase neutrophil numbers in bronchial lavage (Behndig et al., 2006), decrease CO diffusion capacity, and decrease maximum mid-expiratory flow (Pietropaoli et al., 2004). A study in ten Italian cities (Stafoggia et al., 2009) that involve of 275,000 adults carry out that an short-term increases of PM is linked to an of 2.29% increase in respiratory mortality.

In evaluating the literature data are evident the PM effects on human health, in particular related to an increase in cardiovascular mortality and respiratory disease. There are limitations to much of the available PM research. Most epidemiological studies do not use individual exposure data but they use air monitors as surrogates for individual exposure. Despite these limitation different types of studies find a dose-response relationship between PM exposure and adverse effects. While studies show a relationship between PM and adverse health affects, the real mechanism of interaction and the biological pathway that cause these effects has not yet been elucidated.

Because for reasons of methodology, it is inherently difficult to attribute these harmful effects on human health to the individual pollutants. Although it is widely proven that fine particulate is the most responsible for pathophysiological level, the contribution, single or combined, of other pollutants (eg, nitrogen oxides, carbon monoxide, etc.) must be held in account. As shown by the data in the literature the majority of the information on the effects of PM on human health are derived from epidemiological studies, or to a lesser extent, on experimental studies in vivo or in vitro.

So, in parallel to these studies,it is important to implement computational models for the study of molecular interactions that occur among the components of atmospheric particles and that give rise to receptors and signal transduction leading to effects on human health, Given the specificity and temporal and spatial variability of particulate matter is important to assess the specificity and selectivity of individual proteins. Being able to perform these tests requires high experimental economic resources, to overcome this problem it is important to implement a computational strategy for the evaluation and analysis of the molecular mechanisms. Computationally this type of simulations require long timescales of traditional infrastructure so it is desirable to develop new infrastructure to reduce the time of calculation.

The article *Homology Modeling, Docking Studies and Molecular Dynamic Simulations Using Graphical Processing Unit Architecture to Probe the Type-11 Phosphodiesterase Catalytic Site: A Computational Approach for the Rational Design of Selective Inhibitors* describe a computational approach based on homology models, docking and molecular dynamics sim-

ulations to derive a 3D model predictive of PDE11. This work underlines the importance of strategies for the screening of ligands and in the assessment of the interactions to evaluate the effects due to the specificity and selectivity of the ligand-protein interaction. In particular the implementation of a GPU infrastructure permits to simulate long molecular dynamic that enable to highlight the key residues of interaction between the Phosphodiesterase and the ligand, so using this protocol is possible to studies different receptor and let know the principal residues involved in the interaction and develop specific ligands that better interact with the protein.

As noted by literature studies, some effects of PM are due to its passage into the blood stream, in particular it is associated with alterations in circulating levels of coagulation-related parameters such as serum levels of fibrinogen, von Willebrand factor, factor VIII and protein C. So it is important to assess the molecular interactions that are generated in the blood fow to assess the possible effects of particulate air pollution, and this highlights the need for experimental problems in the evaluation of interactions and formation of protein complexes.

This is the context of the work: *Molecular dynamics and docking simulation of a natural variant of Activated Protein C with impaired protease activity: Implications for integrin-mediated antiseptic function.* In this paper has highlighted the importance of an infrastructure performance and has illustrated a protocol for a computational study on the functional activity of the protein C, which involved the creation of various docking simulation to better understand the protein interaction and the need of the definition of a new scoring function

that included biological information of the interaction of the protein in addition to the energies of docking to better ranking the results of docking.

In addition to the effects on the circulatory and respiratory system are important the effects on the endocrine system. The effects on the endocrine system are due to endocrine disrupting chemicals (EDCs), with this term refers to a broad category of substances mainly, but not only, of artificial origin, which are able to bind as agonists or antagonists to the receptors of various hormones. Endocrine disruptors are substances that then interfere with the synthesis, secretion, transport, binding, action or elimination of natural hormones in the body, responsible for the development, behavior, fertility, and maintenance of cellular homeostasis (DiVall, 2013; Buyukgebiz, 2012).

These compounds can cause serious damage to exposed organisms, but often aren't immediately apparent because at low doses there aren't acute toxicity, and may, in the case of large environmental exposures produce effects at the population level. Many of the pollutants that are objects of deep environmental and toxicological studies are EDCs. Epidemiological and experimental studies suggest that EDCs may increase the risk of cancer, metabolic disorders, reproductive and developmental disorders.

It is extremely importance their interaction with nuclear hormone receptors (NHRs), in facts these receptor regulate cognate gene networks involved in key physiological functions such as cell growth and differentiation, development, homeostasis or metabolism (Laudet et al., 2004, 2006) Human NHRs are a family of 48 transcription factors, very preserved in term of structural and functional features; many of NHR have been

shown to be activated by ligands.

These evidences motivate the need to provide a system for the assessment of the interaction of various xenobiotics with nuclear receptors, an preliminary tool has highlighted in the work *Nuclear Receptor Database Evaluates the effects of the EDC on the Endocrine System*, which shows an in silico protocol for the preliminary assessment of the interactions between pollutants, particularly EDCs, and nuclear receptors.

# CHAPTER 2

# VERTICAL PROFILES AND OPTICAL PROPERTIES MODEL

The aerosol chemical composition is responsable of the adverse effects on the environment. So to understand the particulate air pollution effects is important to evaluate the chemical composition and its distribution according to the height above the ground. This is the context of the study on the *Impact of aerosols and Black Carbon over Italian basin valleys: from high resolution measurements of vertical profiles to the modelling of radiative forcing and heating rates.* In this study has been presented an high resolution vertical profile of aerosol radiative forcing and atmospheric heating rates. This protocol is based on measurements of vertical profiles of aerosols and of Black Carbon at high spatial resolution that have been obtained by means of a tethered balloon. The tethered balloon

has been equipped with a micro-Aethalometer, an optical particle counter (OPC), a cascade impactor and a meteorological station. The colleted data have been input into a computational model in order to obtain radiative forcing and atmospheric heating rates.

## 2.1 Introduction

Among the whole aerosol constituents, Black Carbon (BC) plays a crucial role as it is reported to be the second most important human emission in terms of its climate forcing (Bond et al., 2013). Moreover the BC affects the climate both warming the atmosphere and, at the same time, cooling ("masking") the surface (Chakrabarty et al., 2012). The wide range of BC-DRE value is due to different reasons: the whole complexity of aerosol chemistry (i.e. mixing state) (Ramana et al., 2010), the surface albedo (Seinfeld and Pandis, 1998) and more important, the spatial heterogeneity in terms of concentrations (horizontal and vertical) due to its low (compared to CO2) lifetime (about 1 week) (Samset et al., 2013; Cape et al., 2012). Recent modeling of the BC-DRE (Samset et al., 2013; Zarzycki and Bond, 2010) evidenced opposing behaviours, with a DRE effect mainly located in the lower or in the upper troposphere depending on the BC location along the profile. The resulting overall degree of uncertainty attributable to the assumptions about the vertical distribution of BC was estimated to be in the range 20-50%.

Moreover, the vertical heterogeneity of BC and its DRE influences the atmospheric thermal structure with heating rates differentiated along height within a range of about 0.5-2 K

day-1 (Chakrabarty et al., 2012; Ramana et al., 2010; Tripathi et al., 2007) as a results different kinds of feedback can take place, such as those on regional circulation systems (i.e. monsoons) and on Planetary Boundary Layer (PBL) dynamics (Ramanathan and Feng, 2009). Currently, there are few experimental data due to the excessive cost especially when conducted using aircrafts (McMeeking et al., 2010; Schwarz et al., 2006) even if, other direct methods, such as tethered balloons and UAVs, can be used to collect long-term measurements at a reasonable cost (Ferrero et al., 2012; Corrigan et al., 2008; Maletto et al., 2003).

Moreover, airplane measurements cannot provide data in the first hundreds meters above the surface, where most of the emissions and boundary layers phenomena take place. There is a clear need to improve the knowledge about aerosol vertical profiles especially over Europe where a plethora of different territories and situations are present. Moreover, the complex orography of Italy represents an interesting and significant case study for black carbon and aerosols monitoring in complex-horography regions. The Italian territory results in a multitude of basin valleys of various sizes, in which urban and industrial centers usually lie. These valleys represent important areas where low wind speeds and conditions of atmospheric stability are common, thus promoting the formation of strong vertical aerosol (and BC) gradients in the lower troposphere (**?**Ferrero et al., 011b; Carbone et al., 2010).

In this work we want introduce indication of the possible feedback induced by BC concentration in the lower troposphere calculating DRE and heating rates along vertical profiles from the aerosol properties and the relationshion between

BC vertical distribution and mixing height (MH) dynamics.

## 2.2 Results and Discussion

In study the BC vertical profiles and aerosol distribution were mesured over three Italian basin valleys with the aim to obtain the characterize the aerosol and BC dispersion under similar orographic conditions. Furthermore the variation of BC concentration and BC aerosol fraction along height appears to be correlated with variations in aerosol optical properties, radiative forcing and heating rate. Right now the knowledge of as the BC DRE depend on the BC vertical distribution is scarce. In this work we underline the BC vertical distribution in relation to the MH.

The analysis shown higher BC concentrations were found close to the ground in all the three sites (Figure 2.1). In particular this ground-level layer affected the first 50-100 m of atmosphere generating a BC concentration increase of +34.2% (TR), +17.3% (MI) and +16.1% (ME) compared to the average BC concentration measured within the whole mixing layer. These BC concentrations near ground-level, are related to the proximity to combustion sources (traffic, heating, industry) (Trompetter et al., 2013). Moreover, this common behavior is of particular importance because it belongs just to BC and was not observed for the whole aerosol; thus, it further enhances the aforementioned vertical changes in the BC aerosol fraction with height.

Another important aspect that can be deducted from Figure 2.1 is that the BC concentrations measured AMH were found quite similar among the three sites and a decrease of BC

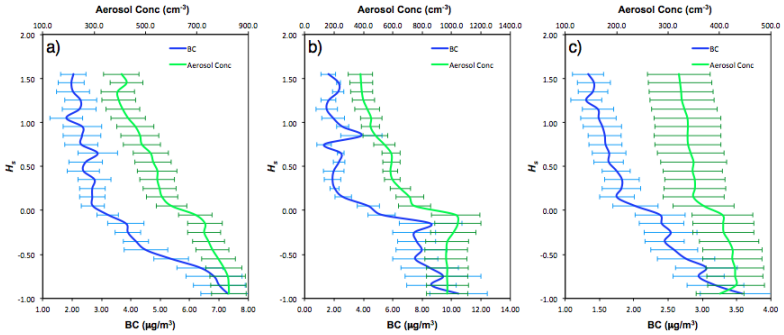


***Figure 2.1:*** *The statistical mean profile of BC and aerosol concentrations along standardized height Hs for Terni (a), Milan (b) and Merano (c).*

variance with height was present in each site. These evidences point to the presence of a relatively constant background value for BC.

The optical properties calculations along vertical profiles require the knowledge of the whole aerosol chemical composition along height. As shown in Figure 2.2 the BC franction decrease from the ground concentration to AMH, contrariwise the OM fraction increased with height.

The ions composition are crucial in determining the aerosol optical properies beacuse, as reported in Ramana et al. (2010) the ratio of BC to scattering species (i.e. SO42-) influences the solar-absorption efficiency. Moreover, the same scattering species (i.e. SO42- and NO3-) also influence the DRH at which aerosol water uptake starts, corresponding to a phase change for the aerosol water-soluble compounds which dissociate going from solid to liquid(Martin, 2000; Seinfeld

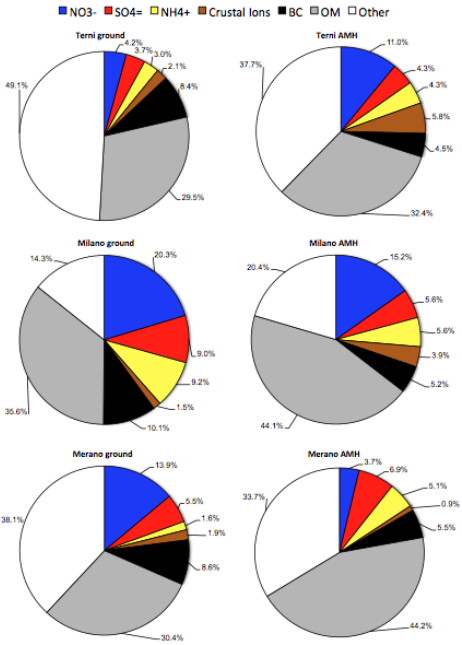


***Figure 2.2:*** *Aerosol chemical composition, determined at ground (BMH) and AMH for TR, MI and ME. Data shown are the respective aerosol mass fraction of each individual aerosol species.*

and Pandis, 1998; Potukuchi and Wexler, 1995); thus DRH is of fundamental importance to assess the final aerosol optical properties (Di Nicolantonio et al., 2009; Randriamiarisoa et al., 2006).

To accurately predict the aerosol DRH we use the E-AIM Model II considering the H+, NH4+, SO42-, NO3-, carboxylic acids, H2O composition of the aerosol. BMH values for TR, MI and ME were close each other and were 64.5%, 67.0% and 65%, respectively. This results is consistent with values mesured at ground-level in MI by means of an Aerosol Chamber (Ferrero et al., 2013). AMH values of DRH estimated for TR, MI and ME are 55%, 62.5% and 67%, respectively. The lowest and the highest values were found over TR and ME due to an increase in the nitrate and sulphate fractions, respectively; as Potukuchi and Wexler (1995) have pointed out, an increase in the nitrate (sulphate) fraction leads to lower (higher) DRH.

## 2.3 Conclusion

The results obtained have allowed to clearly identify the mixing height (MH), which was characterized by a strong vertical concentration gradient of both BC (range: -48.4±5.3% - -69.1±5.5%) and aerosol (range: -23.9±4.3% - -46.5±7.3%). The behavior of the BC in relation at the MH is relevant: above the MH the percentage decrease of BC was higher than that measured for aerosol and thus, the BC fraction of aerosol fell (range: -33.2±4.9% - -47.5±7.9% ) while a shallow BC layer of higher concentrations (range: +16.1% - +34.2%) was found close to the ground, in the first 50-100m of atmosphere, due to the proximity of BC sources.

The obtained results were similar over the three sites and pointed towards a common aerosol dynamics over basin valleys characterized by similar atmospheric stagnant conditions. These data represent the first high resolution vertical profile of aerosol radiative forcing and heating rate obtained over Italy and Europe allowing to describe with detail the radiative forcing induced by BC and aerosol in the lower troposphere, across the mixing layer and within it, where the antroposphere is located.

# CHAPTER 3

# CORROSIVITY OF PARTICULATE MATTER

An important aspect of particulate air pollution is the electrical behavior of aerosols, in particular, one of the critical parameters is the relative humidity of deliquescence (DRH) of particulate air pollution. The ionic component goes into solution for relative humidity values that exceed the DRH, forming a saturated aqueous solution conductive. The characterization of the ionic fraction is therefore crucial to understand the effects on the electrical properties of conductivity of the aerosol.

The atmospheric corrosion has a significant impact on the environment since almost all human artifacts is constantly in contact with the Earth's atmosphere, both in indoor and outdoor environments. The corrosion affecting so many fields of human activity from the scope of construction to electron-

ics, from the preservation of artistic and monumental in many other contexts.

Is in this scenario that fits the study conducted on a DC, for the Italian National Hydrocarbon Institution (GDC-ENI at Sannazzaro de' Burgondi, Po Valley). The study aimed to optimize a DFC operating cycle to save the largest amount of energy and to prevent, at the same time, aerosol corrosion. This goal was reached through the determination of the most reliable thermodynamic limits (especially moisture) based on in-situ measured aerosol properties.

The aerosol properties (number size distribution, chemical composition, DRH, acidity) and meteorological parameters were investigated using reliable and shared methods, characterized by reasonable costs: a situation able to promote this experimental design as a "standard protocol" applicable in similar situations for any DC to estimate its economic and environmental costs in feasibility studies. The investigated aerosol properties determined the potential levels of aerosol entering the DC (equivalent ISO class) and its DRH allowing to choose both the appropriate filtering system (MERV13 filters) and the best thermal cycle (60% of maximum allowed RH) applicable to the DFC. Then, the GDC-ENI operating cycle was investigated showing that the aforementioned choices allowed to reach the indoor ISO-8 standard required by ASHRAE itself. The energy consumption of the DC was investigated revealing an energy saving of 81% compared to traditional AC cooling systems.

## 3.1 Introduction

Data centers (DC) alone are responsible for about 18% of electricity use in Western Europe. The global DC electricity demand increse from 0.5 % in 2000 to 2 % in 2010 (Shehabi, 2009). A traditional data center's cooling system is based on AC units that cool the hot air produced by the IT and then make it available again through a closed-loop air cycle (Shehabi, 2009). Thus, the high energy consumption of DC is due, for a significant fraction (35-50 %), to the cooling process of the IT; other energy sinks are IT (50-60%), energy losses (5%) and lighting (1 %) (**?**). Thus, these kind of AC-DC are characterized by high values of the Power Usage Effectiveness (PUE: the ratio of total data center electricity load to IT electricity load); a PUE ratio of 1.0 indicates that all the energy consumption is due to IT equipment alone while, a PUE equal to 2.0 indicates that cooling, lighting and energy losses are responsible for an equivalent energy consumption of IT. Traditional AC-DC have PUE close to 2.0 (Shehabi, 2009). As a consequence, solutions able to offset their financial and environmental costs (greenhouse gas emissions) are required. In this respect, the need to reduce CO2 emissions has led the EU to define environmental policies.

The need to reduce both energy consumption, in order to comply with the new regulations and economic and environmental costs, push to towards innovative technologies. Moreover, the reduction of cooling process costs is a widely shared target. DFC systems could be use for this purpose: outside air is used to directly cool the IT (Shehabi et al., 2008). However, this approach involves the risk to introduce outdoor aerosol which can become electrically conductive if the surrounding air

reaches the aerosol Deliquescence Relative Humidity (DRH); this process can cause bridging and corrosion that can damage the IT (Shields and Weschler, 1998; Lobnig et al., 1994).

No studies have been conducted to design a DC by starting from the knowledge of the aerosol properties measured directly in situ. In this study we illustrate the design of a DC created for the Italian National Hydrocarbon Institution (ENI) (5200 m2 of IT installed) which is currently under construction and will become operational in December 2013 (Eni web site). The study was based on measured aerosol properties, in order to reach the energy-saving target by means of a DFC system. DFC operating cycle was adapted both to comply with the aerosol guidelines (, TC,T) and to prevent aerosol corrosion.

## 3.2 Methods and Materials

The object of investigation is the ENI Green Data Center located in the middle of the Po Valley (Italy) at Sannazzaro de' Burgondi (SdB). The building have four rooms for Standard Computing (SC, 800 m2 each of IT installed) and two rooms for High Performance Computing (HPC, 1000 m2 each of IT installed). A total area of 5,200 m2 of IT is planned. A DFC for the GDC-ENI is planned: outside air enters the building at floor level, passes through the IT to maintain a temperature set-point of 25°C, and exits through the roof by means of a chimney effect. This system allows to remove the expected rise in air temperature: 12°C in the SC rooms and 20°C in the HPC rooms.

To solve the potential problem of aerosol contamination within a DC together with energy saving the ASHRAE (Amer-

ican Society of Heating, Refrigerating and Air-Conditioning Engineers) Technical Committee 9.9 published guidelines concerning the thermodynamic limits and the aerosol contamination in DC (, TC,T). However these guidelines are general and do not take account of the aerosol chemical and deliquescence properties at the investigated site. Thus we developed an experimental procedure with the aim of supporting the design of a DC working with a DFC system.

The aerosol number size distribution was monitored over time (1 min time res) through an Optical Particle Counter Tandem system (TOPCs: 2 Grimm 1.107 "Environcheck"; 31 size classes, from 0.25$\mu$m up to 32 $\mu$m). This system allowed measuring the "dry" and "wet" aerosol number size distribution. The "dry" size distribution allowed to assess the aerosol pollution level at the location of the GDC-ENI and to simulate the expected indoor concentration under DFC application following the method reported by Nazaroff (2004) and Shehabi et al. (2008) PM1 and PM2.5 were sampled every 4 hours and 8 hours, respectively using a FAI-Hydra dual channel low-volume sampler and chemically analyzed by means of ion chromatography (**?**). The following ions were analyzed: Na+, NH4+, K+, Mg2+, Ca2+, Cl-, NO3- and SO42- together with mono and dicarboxylic acids (formiate, acetate, propionate, oxalate, malonate, succinate, glutarate). The aerosol chemistry was used as an input parameter to calculate the aerosol DRH.

Aerosol DRH was estimated using the thermodynamic Aerosol Inorganic Model (E-AIM Model-II) by **?**: a state-of-the-art thermodynamic model for the H+, NH4+, SO42-, NO3-, carboxylic acids, H2O aerosol system (Hueglin et al., 2005;

Pathak et al., 2004). The outdoor aerosol chemical composition were used as inputs for the model to determine the most restrictive thermodynamic limits within which the worst DRH occur to optimize the DFC operating cycle for the GDC-ENI. In order to validate the E-AIM DRH estimation, the E-AIM hydration curve was compared with that of TOPCs. Moreover an Aerosol Exposure Chamber (AEC) had been specifically designed at the University of Milano- Bicocca for studying the aerosol hygroscopicity. It is a 1 m3 chamber in which is possible to control the thermodynamic conditions. Within the AEC, it is possible to house up to six PM filters over special PTFE supports provided with a pair of electrodes each. The aerosol hygroscopicity is studied by means of conductivity measurements carried out on each filter as a function of the relative humidity (1% RH step). Humidity in the AEC was increased by means of evaporation unit filled with ultrapure water (Milli-Q). Conductivity measurements were carried out using the Hewlett-Packard 3421A acquisition module, while a T and RH were monitored using LSI-Lastem sensors. Measurements were conducted at 25°C, the temperature set-point of IT within the GCD-ENI, on PM2.5 samples. The aim was to verify if the E-AIM model rightly estimated the aerosol DRH.

## 3.3 Results and Discussion

Spring (24/03/2010-19/04/2010) and summer (10/06/2010-10/07/2010) campaigns were conducted at SdB to measure aerosol properties such as number size distribution, chemical composition and meteorological parameters. These data show an overreached the ISO-8 standards, for 74% and 55% of the

time, and were 8.3±0.4 during spring and of 8.1±0.4 during summer.

Thus the GDC-ENI needed a filtering system to maintain the ISO-8 standard levels. Particularly, the filtering systems was designed composed of 456 MERV13 (Minimum Efficiency Reporting Value) filters (total filtering surface of 165 m2 with a maximum flow rate of 2763 m3 h-1 for each filter). The global MERV13 filter efficiency is lower than 100 % and increase with particle size, up to 100 % at 3 $\mu$m (Nazaroff, 2004). Thus, the chemical properties of PM1 and PM2.5 samples, smaller than the 100% size-efficiency of the MERV13 filters were investigated. PM chemical composition showed that the ionic fraction was on average the 32±3% of PMx mass during both campaigns, and NO3-, SO42- and NH4+ accounted for 90-95% of the whole ions while, other cations (i.e. Cl-, K+, Na+, Mg2+, Ca2+) and carboxylic acids accounted about 2% of PMx mass. The ionic component can damage the electronic equipment after solubilisation at the DRH. Thus the E-AIM model was applied to each PMx sample to estimate the DRH values, which were found to fall within a broad range of 40-80% for both PMx. Within this range, the most abundant DRHs were to be found in the 60-65% range, with a frequency percentage of 39 % and 43% for PM1 and PM2.5 respectively.

As a result, the average DRH for PM1 was 61.2±1.1% (spring), and 68.4±1.4 % (summer), while in the case of PM2.5 it was 60.8±0.7% (spring) and 62.4±0.9% (summer). Lower DRH values during spring reflected the influence of aerosol chemistry: NO3- was predominant during spring (17-20% of PMx mass), while SO42- during summer (10-18% of PMx mass); NH4+ remain fairly constant during both campaigns

(4-7% in both cases). This PMx chemical composition is close to that reported in literature for the Po Valley (Perrone et al., 2012; Daher et al., 2012) and turns into changes of the sulphate to nitrate ratio [SO42-/(SO42-+NO3-)] and the ammonium to hydrogen ratio [NH4+/( NH4++H+tot)] along time. Potukuchi and Wexler (1995) showed that for a fixed ammonium to hydrogen ratio, an increase in the sulphate to nitrate ratio (i.e. summer conditions) leads to higher DRHs.

The measured PM chemical composition showed higher sulphate to nitrate ratio during summer (0.72 ± 0.03 and 0.59 ± 0.03 for PM1 and PM2.5) than in spring (0.33 ± 0.03 and 0.20 ± 0.02 for PM1 and PM2.5) while the ammonium to hydrogen ratio remained fairly constant (0.95 ± 0.01 for PM1 and 0.95 ± 0.01 and 0.84 ± 0.01 for PM2.5 during both campaigns). Due to the crucial role of estimated DRH values in optimizing the design of the GDC-ENI DC, the obtained E-AIM output were validated through the use of TOPCs data and from experiments conducted on PM2.5 samples in AEC.

E-AIM values agreed with those estimated using TOPCs; R2 between TOPCs and E-AIM were 0.97 and 0.85 for PM1, in spring and summer, and were 0.98 and 0.95, for PM2.5. Moreover, the AEC (specifically designed at the University of Milano-Bicocca) was used to measure, at 25°C, the aerosol hygroscopicity on 15 PM2.5 samples with the aim to validate if the E-AIM model rightly estimated the aerosol DRH. Figure 3.1 shows an experimental PM2.5 hygroscopicity measurement (AEC data) compared with the E-AIM predicted moles of condensed water versus RH. Considering the whole PM2.5 ensemble, the averaged DRH estimated via E-AIM was 62.8±2.0% in keeping with the values measured using the

AEC: 62.6±1.2%. These results show the reliability of using E-AIM to derive aerosol DRHs, and also are comparable to that estimated at SdB during the sampling campaigns.

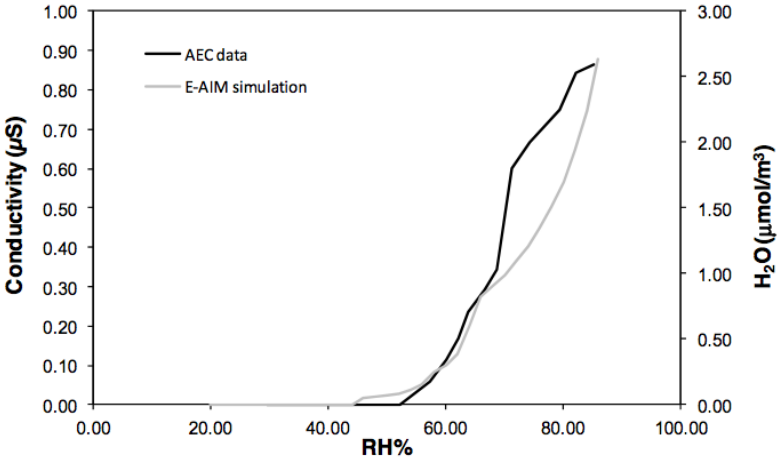


***Figure 3.1:*** *Aerosol hydration curve measured on a PM2.5 sample and predicted by E-AIM (Model II) application.*

Given the validation of DRH calculation, the DRHs values were used to optimize the DFC operating cycle. Estimated DRHs values at SdB were higher than the RH limit "recommended" by ASHRAE (2011) (54 %: 15 °C dew point at 25 °C) and it was lower than the "allowable" limit (80 % of RH). Moreover, all the averaged DRHs were found to be slightly higher than 60% allowing choosing 60% of RH as the upper limit for the DFC operating cycle to prevent a corrosive effects of the aerosol. Results evidenced that both during

spring and summer, C1 and C2 attained the ISO-8 standard. C3 equalled zero because MERV13 filter efficiency reach the 100% yet at 3 $\mu$m (re-suspension was also neglected in the model). The balancing between the external air supply (QS) and the re-circulated one (Qrec) along time allowed to estimate the energy consumption of the GDC-ENI and its PUE. A PUE equal to 1.2 was found, lower than traditional AC data centers (PUE=2.04; Sullivan, 2009), and of other DCs adopting DFC (PUE=1.42-1.46; Shehabi, 2009). This PUE value turns into an annual energy saving of 81% compared to traditional AC data centers (PUE=2.04): 7.4 MWh for 1 kW of installed IT and 221 GWh for the entire GDC-ENI. The annual energy saving, compared to other DCs adopting DFC system (PUE=1.42-1.46), was also relevant: 55% (2.1 MWh for 1 kW of installed IT and 63 GWh for the entire GDC-ENI). In terms of environment savings t of CO2 not emitted were estimated considering a CO2 emission factor of 362 gCO2 kWh-1 (European Environment Agency, EEA. Results evidenced an emission savings for each kW of IT: 2.7 t of CO2 (80 kt the entire GDC-ENI), compared to traditional AC data centers (PUE=2.04) and 0.8 t of CO2 (23 kt for the entire GDC-ENI), and compared to other data centers adopting DFC systems (PUE=1.42-1.46).

## 3.4 Conclusion

Cooling systems are among the key factors to the high energy demands of Data centers (DC). The energy request of Air Conditioning (AC) could be reduced using a Direct Free Cooling (DFC) system that uses the outside air to directly

cool the information technology (IT). On the other hand this approach involves the risk to introduce outdoor aerosol that can be electrically conductive and cause damage to the electronic equipments, if the air reaches the aerosol Deliquescence Relative Humidity (DRH). This work reports results regarding a-priori study conducted on a DC and the results underline the possibility to use a DFC if the filtering system and the best thermal cycle are choose appropriately, this leads to an energy saving of 81% compared to traditional AC cooling systems.

# CHAPTER 4

# DESIGN OF SELECTIVE INHIBITORS

In the assessment of the effects of particulate air pollution on human health is important to evaluate the molecular interactions that occur. Of particular relevance assess the specificity of individual proteins. This type of feedback is to be economically burdensome from an in vivo or in vitro experimental point of view, then it becomes important to the implementation of a computational strategy for better understanding these mechanisms, and reduce the economic efforts. From the computational point of view these tests are time consuming, so it is desirable to develop new infrastructure to break down the timing of the calculation.

In this context includes the study of phosphodiesterases: *Homology Modeling, Docking Studies and Molecular Dynamic*

*Simulations Using Graphical Processing Unit Architecture to Probe the Type-11 Phosphodiesterase Catalytic Site: A Computational Approach for the Rational Design of Selective Inhibitors*. Cyclic nucleotide phosphodiesterases (PDEs) are enzymes that regulate cellular levels of cAMP (cyclic adenosine monophosphate) and cGMP (cyclic guanosine monophosphate) through hydrolysis of these second messengers. Different members of this family have been discoverd as yet and they differ by kinetic properties, specificity of substrate and inhibitors, tissue distribution and sequence-derived information (M. and J., 2007); the latest family's element discoverd is the PDE11 (Hetman et al., 2000). Consequently the PDE appear to be a case study interesting for the screening of the interactions and effects due to their specificity and selectivity. In this case study we describe a computational approach based on homology modelling, docking and molecular dynamics simulation to derive a predictive 3D model of PDE11. The computational complexity of the analysis required also setting up a new infrastructure which would use the GPU than the CPU out to be much more efficient, as shown in Figure 4.1;

## 4.1 Introduction

The PDE family is characterized by structural determinants such as: a catalytic domain (270 aminoacids length); a regulatory domain, an allosteric cGMP binding sites, a phosphorylation sites, phosphatidic binding site, PAS domain, autoinhibitory sequences and membrane association domain and a domain for the action of MAP Kinase. The domains have different importance between the PDE's members. The major

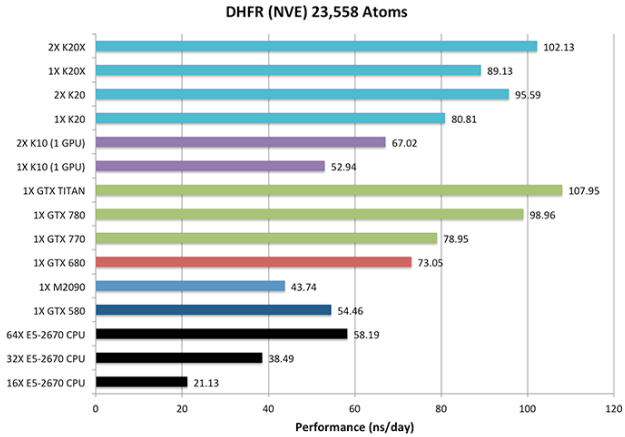


***Figure 4.1:*** *Examples of a single run of Amber molecular dynamics on one or more GPUs and one or more nodes*

conserved domain is the catalytic domain with a 20-45% identity among family and represents the core of PDE structure. In this domain are present consensus metal binding motifs: a $Mg^{2+}$ binding motif related to metal-ion phosphohydrolases and two $Zn^{2+}$ binding motifs (Francis et al., 2001).

Each PDE is encoded by a minimum of 1 to a maximum of 4 distinct genes for a total of 20 genes in mammals. Moreover there are alternative splicing and/or multiple promoter that increase the number of probable different protein to 50. This large number of protein may permit a specific intracellular localization and inducing a inducing fine-tuning of compartmentalized regulation for cAMP and cGMP. Phosphodiesterase 11 (PDE11) is the latest isoform of the phosphodiesterase family

to be identified, acting on both cAMP and cGMP. The tissue distribution of PDE11 has not yet been fully defined, but primarily has been reported in skeletal muscle, prostate, testis and salivary glands. The PDE11 catalytic domain is closest to PDE5 with a 50% identity and 71% similarity (Fawcett et al., 2000). The similarity between PDE11 and PDE5 is also demonstrated by the fact that several PDE5 inhibitors reacted with PDE11. This family is relevant as potential therapeutic target for the treatment of various caridac pathologies, as recently reported in literature (Miller and Yan, 2010).

In 2009, Francis and co-workers investigated the role of the invariant Gln (Gln869) as a determinant of substrate and inhibitor affinity using mutagenesis (Q869A), cGMP analogues, and a battery of cyclic nucleotide (CN) analogues to map features of the PDE11 catalytic site. As result a PDE11 inhibitor, such as tadalafil, showed affinity to Q869A 137-fold weaker than that of WT PDE11 (Weeks et al., 2009). More recently, Hoffman and co-workers tested different compounds against the PDE1-11 enzymes (Ceyhan et al., 163) and had shown that some compounds proved to be PDE11 selective inhibitors, inactive towards the PDE5 enzyme and on the other hand only a specific compound has had action also on PDE5.

The structure of PDE11 is not well defined, in fact at right now there aren't experimental data about PDE11 X-Ray structures, so we applied a computational approach that uses tecniques of homology modelling, docking and molecular dynamics simulation studies with the aim to most understanding of the enzyme-inhibitor interactions.

The first step is to obtain a PDE11 model structure; this model is built from the Xray structure of the PDE5/Tadalafil

complex (pdb code 1XOZ). The selection of the mold template is crucial for the correct behavior of the model, so we use a PDE5 complex with an inhibitor that we know interacts with PDE11. The model was create by applyng the ligand-based homology modeling strategy proposed by Moro et al. (2006) and the both steps of model building and refinement are performed with the presence of the ligand to guide the specific steric and chemical features. Another aspect to take into account is derived from Wang et al. studies (Wang et al., 2006), these studies underline two conformational variants that occured at the H-loop (residues 660-683) and M-loop (residues 788-811) when the PDE5 is in complex or is unbound. In particularly the H-loop is important for the recognition of the substrate so we must considered also the H-loop conformation in the realization of a very realistic 3D model of the enzyme.

Once completed the model is important validate the structure obtained, for this purpose we made simulations with inhibitors of both PDE5 and PDE11 with the aim to assess whether our model is in agreement with the experimental data. Following this procedure we could therefore hypothesize the suitability of our model for studies "in silico". More studies with other compounds can permit to point out the most relevant features of a PDE11 inhibitor and provide guidelines for the synthesizing a new one

## 4.2 Methods and Materials

### 4.2.1 Ligand preparation

All the compounds selected are been taken by literature that show experimental studies with inhibition constants, these

compounds were built and parameterized by Gasteiger-Hückel method and then energy minimized using MMFF94 force field, with root mean square gradient set to 0.00001 (Bairoch and Apweiler, 2000).

### 4.2.2 Ligand-Based Human PDE11 Homology Modeling

The homology model has been generated from an X-ray structure of PDE5 enzyme (PDB code: 1XOZ; resolution 1.37 Å) in complex with tadalafil; we used this structure because the PDE catalytic domain is highly conserved and the ligand is an inhibitor for both PDE. The aminoacid sequence and the 3D structure are been taken from the SWISSPROT database (Bairoch and Apweiler, 2000). and the Protein Data Bank (Berman et al., 2000) respectively. Using MOE software we aligned the amino acids sequence with the corresponding residues of 1XOZ on the guideline of the Blossum62 matrix. The output of the program consists of a set of ten possible models that were independently built on the basis of a Boltzmann-weighted randomized procedure (M., 1992) combined with specialized logic for the handling of sequence insertions and deletions of any selected extra atoms during the energy tests and mini mization stages of the modeling procedure (Fechteler et al., 1995).

The model was create by applyng the ligand-based homology modeling strategy proposed by Moro et al. (2006). This technique is an update of a conventional homology modeling strategy, it take into account of the ligand features during the building of the model. The presence of the ligand in the model building and refinement is important in the considering the in-

hibitor specific steric and chemical features and this technique result very useful when the regions of interaction with the ligand are flexible and specific. The created models are many alike and there were no significant main chain deviations. So the model with the best packing quality function was selected for the further steps.

The energy-minimized structure was obtained by MOE using the AMBER94 force field (Cornell et al., 1995). In particular this step was performed with 1000 steps of steepest descent followed by conjugate gradient mimimization to obtain an rms gradient of the potential energy less of 0.1 kcal/mol/Å. Finally the model was assessed by analyzing the Ramachandran plots.

### 4.2.3 Molecular docking studies

The molecular docking studies were done by Surflex docking module implemented in Sybyl-X 1.0, after this step every best docking pose of every compound was refined by energy minimization(CHARMM27).

### 4.2.4 Molecular dynamics studies

Once you have the final structures of the complexes is important to assess the stability, in particular we done two type of molecular dynamics: one on the unbound PDE11 and the other on the structure obtained from docking experiments. After the molecular dynamics were done an analysis of the interaction patterns with the aim to identify the principal residues of PDE11 involved in the binding.

The simulations were performed using AMBER12 package and the ligand parameters were calculated using the An-

techamber module (Wang et al., 2001) and in particular the empirical charge model AM1-BCC (Jakalian et al., 2002). For the simulations we applied the following protocol that uses the AMBER ff03 force field for the protein and treats the $Zn^{2+}$ and $Mg^{2+}$ ions with the 'non-bonded model' method (Stote R., 1995). The system is neutralized in a 8 Å truncated octahedral box of water by adding sodium ions.

The simulations were performed at a neutral pH and so the histidines 668 and 704 are protonated at $\delta$ position to form coordination bonds with $Zn^{2+}$ ions. The water molecule between $Zn^{2+}$ and $Mg^{2+}$ was treated as hydroxide ion as suggested by studies of Li et al. (2013). Histidines 664, which is nearest to the hydroxide ion, can readily capture a proton and was turned into the protonated histidines. All the bonds involving hydrogen atoms were restricted by the SHAKE algorithm (Shuichi and Kollman, 1992), and the time step was set to 2 fs. The cutoff distance was selected as 8 Å, with long range electrostatic interactions treated with the particle mesh Ewald (PME) method.

The type of simulation requires a large amount of computational time and resources so we have been decided to carry out the simulation on GPU architecture that permit to perform long simulations and find stable interactions involved in the complex with the finally to suggest guideline for the identification and synthesis of potent and selective inhibitors. To perform the simulation we use the PMEMD program a GPU implementation of AMBER12 Sander on a cluster of Tesla K20 Graphical Processing Unit (GPU). This GPU-based computational architecture allows to perform a 50ns molecular dynamics in less than 2 days.

The protocol expected four minimization step, one heating and equilibration step before the production fase, the dynamic fase. During the four minimization step the heavy atoms in the unbound protein and ligand-protein complex were restrained with digressive constraints of 500, 100, 10, and 0 kcal/mol/Å, respectively. These steps consist of 5000 cycles: 2500 cycles of steepest descent minimization and 2500 cycles of conjugated gradient minimization. After minimizations, a less constraint of 10 kcal/mol/Å was applied to restrain all the heavy atoms in the complex during the next two fase of heating and equilibration. The heating step consist of 50ps of Langevin dynamics at a constant volume to heat the system to 300K, the equilibration step consist of 100ps at a constant pressure of 1 atm. The last step of dynamic, the production fase, includes a periodic boundary dynamics simulations of 50 ns with constant pressure at 1 atm and temperature at 300K.

The analysis were performed with the Ptraj module of the AMBER12 package. The parameters analyzed are the the root mean square deviation (RMSD) of the protein backbone and ligand atoms using least-squares fitting. The structures medium extracted from the dynamics were then refined by a step of minimization to obtain the final structure.

## 4.3 Result and Discussion

### 4.3.1 Structural analysis of the human PDE11 model

The catalytic site of all PDEs is highly conserved and it can be subdivided in a metal-binding pocket (M pocket); a solvent-filled side pocket (S pocket); a pocket containing

a purine-selective glutamine; and a hydrophobic clamp (Q pocket) (Card et al., 2004). To explore the hPDE11 catalytic site features, an enzyme homology model had been built using 1XOZ PDE5 as template, by applying the ligand-based homology modeling approach. As shown in Figure 4.2, one docked into the PDE5 catalytic site is engaged in one H-bond with the key glutamine Q817.

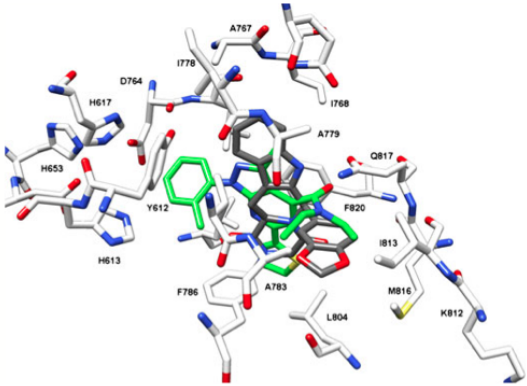


***Figure 4.2:*** *Pose of first compound into the PDE5 catalytic site (1XOZ). The X-ray pose of tadalafil is also depicted. C atoms are colored in green and in gray, respectively. Residues located 5 Å from the compounds are shown and labeled*

The hPDE11 protein model had been derived by the alignment of the hPDE11A (Q9HCR9) fasta sequence on the X-ray co-ordinates of human PDE5 enzyme (1XOZ), on the basis of the Blosum62 matrix implemented in MOE software (Figure 4.3). The reliability of the alignment was verified by the

high value of the pairwise percentage residue identity (PPRI = 46%).

***Figure 4.3:*** *Sequence alignment of the PDE11 catalytic site on the basis of the PDE5 (1XOZ) coordinates.*

The obtained hPDE11 model was superimposed to the coordinates of 1XOZ, used as template for the homology modeling calculations, displaying a quite positive RMSD value (RMSD = 0.173 Å, calculated on the carbon atom alignment). The final model backbone conformation was inspected by Ramachandran plot, showing the absence of outliers in the general psi-phi plot.

### 4.3.2 Molecular dynamic studies

Molecular dynamics were performed to evaluate the stability of the predicted 3D structure of the human PDE11 and of the ligand-enzyme complexes. The analysis of RMSD, calculated respective the initial minimized structure, underline that the human PDE11 model is structurally stable and reaching equilibrium after 10ns of simulation (Figure 4.4).

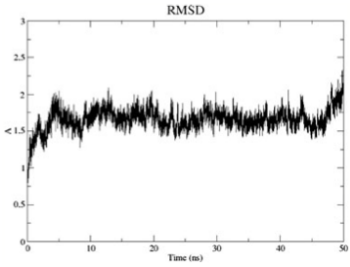


***Figure 4.4:*** *Root mean square deviation (RMSD) profile of backbone of PDE11 model during the MD simulation.*

Another interesting analysis is the Root mean square fluctuation (RMSF) that permit to evaluate the motility of the residues of the protein that show the residues from 711 to 734 and 845 to 859 were the most mobile part of the protein and they were located at the H and M loops (Figure 4.5).

These results suggest a conformational change in that region and this is confirmed by crystallographic studies of PDE5 in bound and no bound form (Wang et al., 2006).

In this study were evaluate the complex of PDE11 with three different ligands and their molecuar interactions with

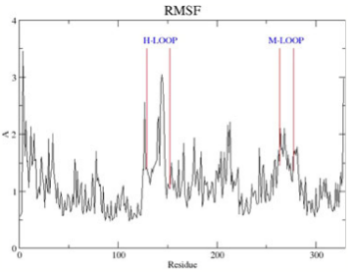


***Figure 4.5:*** *Graphic of RMS fluctuation of residues in PDE11 model during the MD simulation excluding the first 10 ns of equilibration). RMSF residues of H-loop (711T-734D) and M-loop (E845-R859) are indicated.*

PDE; so we performed an RMSD analysis of ligands and backbone as shown in Figures 4.6 and 4.7 where it can be observed that the equilibrium is reached after 20 ns with a RMSD value around 1.7 Å for two compound and an RMSD value of 1.5 Å for the third compound. These result suggest that the third compound is more stable of the other two compound.

Next we analyzed the interaction between the amino acid residues and the different ligands, what emerge is a compound that interacts solely with Q869, while the second compound also interacts with residue W872 and only the third ligand is able to establish hydrogen bonds with all key residues ( Figures 4.8 to 4.10).

Is more important to underline the third compound behavior that show hydrogen bonds with W872 and T835 and a further bond between the nitrogen after 20ns with the ligand and Q869 which however is not stable because after 40ns the

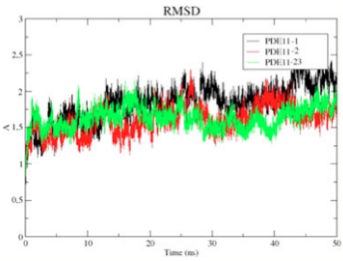


***Figure 4.6:*** *The root mean square deviation (RMSD) of PDE11 backbone of the three studied complexes obtained during MD simulations.*

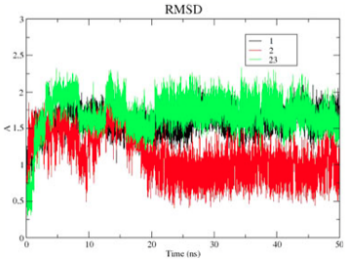


***Figure 4.7:*** *The root mean square deviation (RMSD) of the compounds obtained during MD simulations. RMSD profile suggests that compound 2 is more stable.*

distance increases to 6 Å. At the same time it is observed the formation of another bond between the oxygen atom of the glutamine and the ligand. After further 20ns is observed the change of the hydrogen bond , which suggests that the bond has a swing trend. The same behavior was observed by us for residue D816, as shown in Figure 4.10.

To define the binding mode we extract the average structure from the molecular dynamics and compared with those derived from docking simulation. We can observe that the third compound better occupies the catalytic site (Figure 4.11), infact performs a wider network of hydrogen bonds due to its

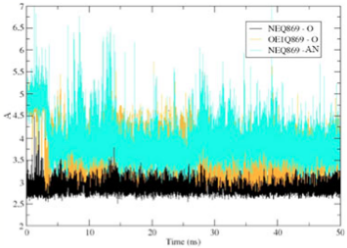


***Figure 4.8:*** *Variation of distances of heavy atoms (donor and acceptor) involved in H-bonds between PDE11 model and compound 1.*

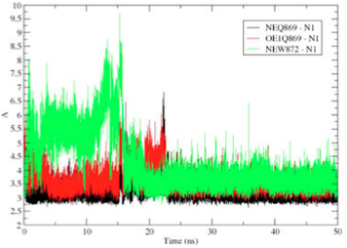


***Figure 4.9:*** *Variation of distances of heavy atoms (donor and acceptor) involved in H-bonds between PDE11 model and compound 2.*

longer scaffold.

## 4.4 Conclusion

In the absence of experimental data about PDE11 X-ray structures, this work highlights the importance of a in silico simulations to gain a better understanding of the enzyme-inhibitor interactions. This approach based on homology modeling, docking, and molecular dynamics simulation has allowed to obtain a predictive 3D model of PDE11. The observation gain from this method permito to obtain useful information for the design of new selective and potent compounds and we thus can reasonably hypothesize that much more potent

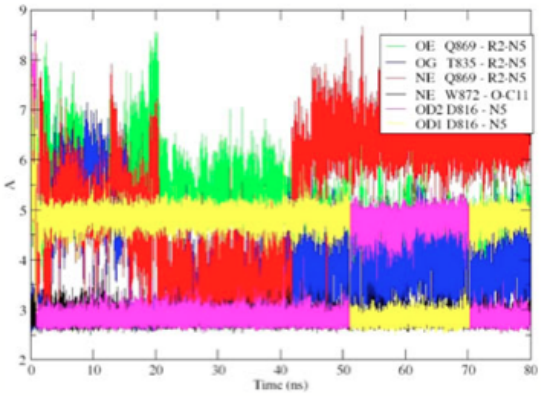


***Figure 4.10:*** *Variation of distances of heavy atoms (donor and acceptor) involved in H-bonds between PDE11 model and third compound.*

and selective PDE11 inhibitors could be designed following a molecular structure simplification strategy, which should take into account the establishment of interactions with the key residue Q869 for PDE11 inhibitory activity, plus interactions with T835, for getting more potent compounds and with the Q pocket V820 and V830 residues, to achieve hPDE11 selectivity. The use of the new GPU architectures helped in speeding the computational investigation and in defining which interactions should be taken into account in the ligand-enzyme binding process allowing long times of MD simulations. This will be useful in the next step of this research, aimed at the design and synthesis of new more potent and selective PDE11 inhibitors.

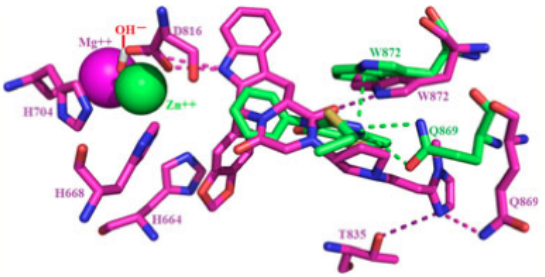


***Figure 4.11:*** *The binding mode of compounds 2 and 23 into PDE11 catalytic domain after MD simulations is depicted. The main residues involved in H-bond are reported and labeled.*

# CHAPTER 5

# ANALYSIS OF PROTEIN FUNCTIONS

Previously we have seen how it is required an infrastructure of highly computational capacity to perform calculations computationally onerous, in other cases the calculations are not computationally burdensome from a point of view of calculation time but by the amount of resources required to run several independent jobs. In this case it is very useful to take advantage of grid computing that allows you to use many computational resources.

One example is the computational study on the functional activity of the protein C, which involved the creation of various docking simulation to better understand the protein interaction. In this work it was also important to the realization of a new scoring function that included biological information of

the interaction of the protein in addition to the energies of docking to better ranking the results of docking.

## 5.1 Introduction

Protein C (PC) also known as autoprothrombin IIA and blood coagulation factor XIV is the central enzyme of the blood anticoagulant pathway. PC circulates in plasma as a single chain zymogen precursor which is activated by proteolytic cleavage of an activation peptide by means of thrombin/thrombomodulin endothelium associated complex.

Activated protein C (APC) exerts its anticoagulant activity through a proteolytic inactivation of coagulation factors V (FVa) and VIII (FVIIIa) with the involvement of several cofactors (Esmon, 2006). In addition, APC has a key role in the regulation of inflammation. It prevents leukocyte rolling, tissue factor exposure, and tumor necrosis factor (TNF) production by monocytes, thrombin-mediated inflammatory actions, and apoptosis of endothelial cells.

In addition, an important role in protecting against sepsis has been attributed to APC (Toussaint and Gerlach, 2009) and its use as a antiseptic drug has arisen a large interest. It has been shown that the antiseptic function is, at least partly mediated by the binding of APC to leukocyte integrins and this interaction inhibits neutrophil migration to infected tissues, thus reducing the damaging effects of sepsis (Oganesyan et al., 2002).

The binding to integrin is made possible by the presence of the typical integrin binding motif RGD at the N-terminus of the APC C chain. The RGD sequence is a well-known motif of

interaction present in proteins involved in cell adhesion such as fibronectin, vitronectin, fibrinogen, von Willebrand factor, thrombospondin, laminin, entactin, tenascin, osteopontin and others.

X-ray structures of $\alpha V\beta 3$ integrin in the unliganded and in complex with a RGD peptide allowed to characterize a specific binding site spanning alpha and beta chains and including divalent metal ions in well defined positions called MIDAS, LIMBS and ADMIDAS (Xiong et al., 2001, 2002).

Comparisons between the unbound and RGD-bound forms, showed that major conformational changes occur upon ligand binding. The peptide binding mode at the $\alpha/\beta$ subunit interface is characterized by a complex network of polar interactions involving negatively charged aspartic acid of the RGD motif that protrudes into the protein interior and establishes contacts with Ser 123, Asn 125 of beta subunit and with two Mn++ ions one of which mediates the contact with serine 121 (MIDAS motif).

The RGD's arginine side chain points toward a narrow groove formed by a beta propeller domain in $\alpha$V subunit and establishes a bidentate polar contact with Asp218 and Gln180 (Xiao et al., 2004). Several mutagenesis studies have shown that the mutation of Gly 216 to induced conformational change, the $\alpha$-tryptase ligand binding site is blocked and the proteolytic enzymatic activity is lost (Marquardt et al., 2002; Pereira et al., 1998; Rohr et al., 2006). Prompted by the paradigmatic example of tryptases, we analyzed the structural and functional effects of the mutation of the Gly216Asp in APC by means of molecular dynamics simulation and predicted the ligand binding impairment by docking simulations.

Our study shows that such mutation can result in a folded protein wit impaired protease activity. However, superposition of the integrin binding motifs between wild-type and mutant forms suggests that the interaction with integrin can still occur. Thus, the mutant is likely to retain the antiseptic function related to the neutrophyl integrin binding and hence might still be usable for therapeutic applications.

## 5.2 Methods and Materials

The atomic coordinates of the X-ray structures of APC (PDB: 1AUT) and $\alpha V\beta 3$ integrin (PDB:1L5G) were retrieved from the RCSB Protein Data Bank (Rose et al., 2013). All simulations were performed on the 1AUT C-chain after removing L-chain, Ppack ligand and crystallization water molecules. For protein-protein complex prediction, A and B chains of integrin were used, as they are essential for binding site arrangement, while ligand coordinates and metal ions were removed.

### 5.2.1 Modeling of APC-Integrin complex

The model structure of the complex was obtained using protein-protein docking. The whole procedure is summarized in Figure 5.1: an initial docking pose for the APC-integrin complex was obtained with ClusPro2.0 that performs a rigid-body docking search and clustering-based model ranking (Comeau et al., 2004).

Protein coordinates and calculation constraints consisting of a list of attracting residues, inferred from the $\alpha V\beta 3$-integrin X-ray structure (namely Arg 24 and Asp 26 of the RGD motif

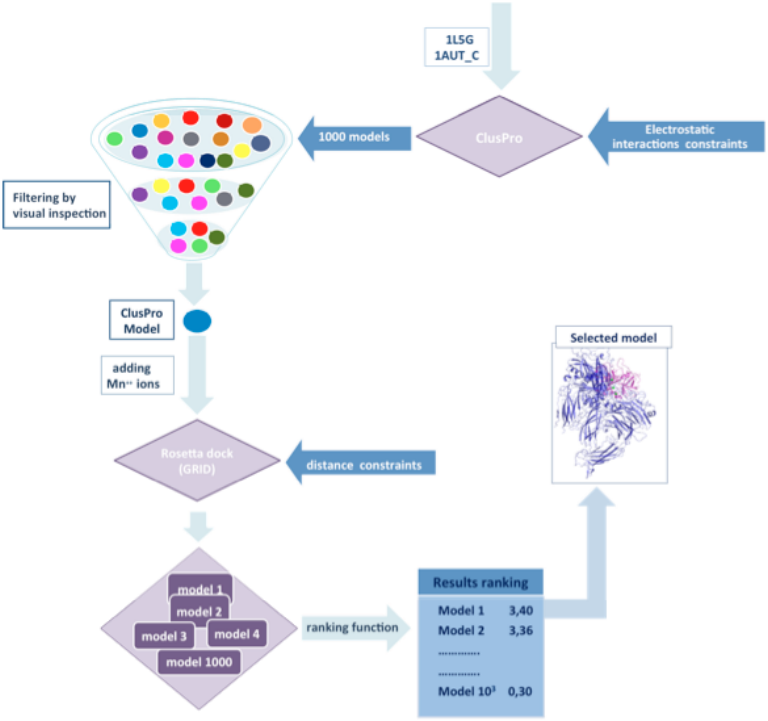


***Figure 5.1:*** *Flowchart of protein-protein docking protocol applied to the modelling of APC-Integrin complex.*

of APC and Ser 121,123 ($\beta$ chain) and Asp128 ($\alpha$ chain) of integrin), were submitted to the ClusPro server (Kozakov et al., 2010). From ClusPro results, we extracted a single pose that satisfied the given interaction criteria.

The selected model was then locally refined using the high-resolution step of RosettaDock v.3.2 (Chaudhury et al., 2011). The method applies random perturbation for rigid-body optimization and rotamer trials for side-chains conformation repacking (Wang et al., 2005). RosettaDock v.3.2 algorithm also permits to incorporate explicit metal ions in the protein structure, also taking into account the metal coordination site of the proteins.

Therefore, we included the coordinates of three manganese ions taken from the X-ray structure of the $\alpha V\beta 3$ integrin binding site. Three distance constraints (APC: Asp26 and $\beta$3-Int:Ser121; Ser123; and APC:Arg124 and $\alpha$V-integrin:Asp218) were set with the purpose to drive the docking procedure toward biologically compatible interactions, using the Rosetta's Gaussian function.

Rosetta simulation was performed on a grid computing infrastructure using an in-house developed software for computation management in EGI. By using a pilot job strategy, the software allowed easy job submission, automatic detection and management of Grid failures, job scheduling with near-to-constant throughput, and other advanced features allowing to carry on the large computations required reliably and with highly predictable completion times.

The RosettaDock output consisted of 1000 models (Figure 5.1) that were ranked using an 'ad hoc' developed scoring function that takes into accounts four terms: the energy of the

complex in kcal/mol and the three interchains distances corresponding to above listed constraints. Each term is rescaled to take values in the range (0,1) where 0 represents the maximum energy and distance values and 1 represents the minimum energy and distance values. The overall score takes values in the range (0,4) where 0 represents the worst and 4 the best conformation.

### 5.2.2 Modelling and Molecular dynamics of G216D mutant

To obtain the initial con conformation of the G216D mutant we solvated the wild-type C protein (1AUT-C chain) in a octahedral solvation box minimized and simulated for 50 ns using version 4.0.3 of the GROMACS software package (Van Der Spoel et al., 2005) using the GROMOS96 force field (Van Gunsteren et al., 1996) and the SPC water model (Berendsen et al., 1081). To extract the correct structure we focusing our analysis on the loop residues 211-218 in order to define the most significantly populated local structure surrounding the mutation site and we introduced the mutation G216D in this cluster. The perturbation is therefore introduced in a locally well equilibrated structure, which facilitates the analysis of the structural change induced by the mutant residue. After that the structure was solvated,minimized and simulated for 50ns with the same procedure of the wild type. The structures of the binding pocket after mutation were analyzed by clustering the trajectory snapshots and focusing on residue stretches 184-193 and 211-226.

### 5.2.3 APC-inhibitor docking simulations

The X-ray structure of Protein C wild type (PDB ID 1aut) and the structure of the mutant obtained by molecular dynamics were used for Protein-Ligand docking studies. PPACK coordinates were obtained from crystal structure of Protein C (PDB entry 1aut). Docking simulations of PPACK inhibitor at the binding site of the Protein C wild type and Gly(216)Asp mutant were carried out using AutoDock Vina (Trott and Olson, 2010).

AutodockTools utility was used to prepare proteins and ligand for docking simulations and to analyze the results. The program adds polar hydrogen atoms to protein and ligand and merges non-polar hydrogen atoms. Then Gasteiger charges are added to all atoms. Protein coordinates were set to be rigid while ligand bonds were set to be rotatable and a grid box of 26x26x22 points, was centered on the enzyme binding site.

The exhaustiveness of the global search was set to 8, the number of generated binding mode was set to 100, and maximum energy difference between the best and the worst binding modes was set to 4. The lowest energy conformation, based on evaluation of AutoDock Vina's empirical scoring function, was accepted as the best complex model.

## 5.3 Result and Discussion

### 5.3.1 APC -Integrin docking complex

The presence of a RGD motif in APC has suggested a role of this serine protease in neutrophil migration. In fact, the binding of APC to different integrin types was demon-

strated (Xiao et al., 2004) by neutrophil migration assay experiments. With the purpose to examine the molecular interactions of APC with the integrin binding site, we modelled the 3D structure of the APC-Integrin complex by a two-step protein-protein docking approach.

A first raw complex that presented an interaction pattern involving at best the key residues of the known RGD-integrin complexes was selected by visual inspection from the models generated by ClusPro2.0. Further RosettaDock refinement returned 1000 complexes falling within an energy interval from -684.21 and -621.45 Kcal/mol, while the distances between the residue pairs Integrin-Ser121/ APC-Asp26, Int-Ser123/APC-Asp26 and Int-Asp218/APC-Arg24 ranged from 10.94 to 9.51 Å, from 10.14 to 6.29 Åand from 6.77 to 5.15 Å, respectively. The results were ranked with a criterion that combined the lowest energy value and the minimum mean distance between the three considered residue pairs.

Application of the described scoring function allowed to select a final model with a score value of 3.4 and an energy value of -679,68 Kcal/mol and a triad of distance values corresponding to 9.51 Å, 6.29 Åand 6.0 Å.

A Connolly surface representation of the final complex is shown in Figure 5.2 a. The shape complementarity between the interacting surfaces indicates a satisfactory packing of the two structures and a correct orientation of the RGD motif toward the integrin binding site extending over the $\alpha$ and $\beta$ chains. Details of the interaction are shown in Figure 5.2 b.

A hydrogen bond is formed between OD2 of Asp218 of $\alpha$ chain and N of Gly of RGD. The aspartic side chain of RGD is pointed towards Ser-123 and the Midas Mn++ ion of

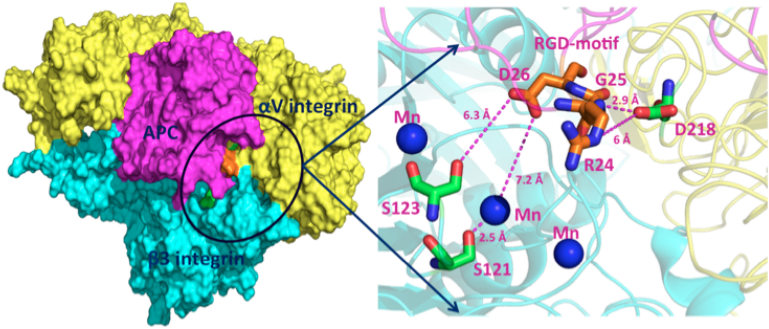


***Figure 5.2:*** *Representation of the best scoring pose of APC on the $\alpha V\beta 3$ integrin. Panel a: Connolly surface representation: the $\alpha$ and $\beta$ chains of $\alpha V\beta 3$ in complex with APC are in yellow, cyan, and magenta, respectively. The region of interaction is circled and integrin residues at the interface are shown in green while apc rgd motif is colored in orange. Details of interaction are shown in panel b: interacting residues are shown in stick representation and coloured by atom type with O atoms in red, N in blue and C atoms in orange and green for RGD-APC and integrin residues, respectively; MN ions are shown as blue spheres. Distances are represented as dashed lines*

integrin $\beta$ chain, suggesting electrostatic interactions between the two interfaces. As expected, the pattern of interaction observed in the integrin-RGD peptide X-ray complexes, could not be reproduced in our model, due to the presence of the surrounding loops that hampers the full exposure of the APC RGD motif.

However, loops flexibility and conformational fitting induced by ligand binding can be reasonably invoked to explain tighter interaction in physiological condition (Teilum et al., 2009). A similar situation has been observed for serine protease thrombin (Papaconstantinou et al., 2005),carrying a RGD sequence in positions 197-189 (on the opposite side of RGD motif of APC) that mediates its interaction with $\alpha$V$\beta$3 integrin. The structure of the thrombin in a non-canonical conformation, exposing the RGD sequence to the solvent, has been solved by X-ray crystallography (PDB code 2A0Q, (Papaconstantinou et al., 2005)). The conformational change was incidentally observed in the attempt to crystallize the protein under peculiar conditions in the absence of inhibitors and at very high salt concentration.

The authors infer from this observation that this previously unseen thrombin conformation is required for integrin recognition. Despite the large amount of observations related to integrin-protein binding, no three-dimensional data are up to now available for a complex of integrin with a whole protein. Thus, our model represents a first attempt to describe the binding mode of a globular protein such as the serine-protease APC with the $\alpha$V$\beta$3 integrin.

### 5.3.2 Molecular dynamics simulation of Gly216 Asp mutant

The G216D mutation was introduced in a previously equilibrated conformation of the wild type protein corresponding to the apo form of the APC enzyme. Subsequently, a 50 ns long MD trajectory of the mutant protein was carried out and analyzed. The overall fold of the mutant protein is maintained during MD (average RMSD 2.1 Å, which is comparable with the average RMSD of the wt simulation 2.7 Å) and also the residue fluctuation profile does not show overall significant changes with respect to the wild type (Figure 5.3A).

However, a notable deviation from the wild type fluctuations is locally observed at loop 1 residues 184-193 and 211-226, which are significantly more flexible in the mutant, as well as at the adjacent loop 150, whose flexibility is reduced in the mutant. This fact suggests a perturbed state of the catalytic site induced by the mutation.

To further investigate this aspect, RMSD and clustering analyses were carried out by focusing on the binding pocket during the dynamics. The RMSD shows a structural transition at about 15 ns, which leads to a stable conformation of the binding pocket (Figure 5.3B). The clustering analysis on the same region confirms that, after a transient, the structure converges to a structurally stable conformation after 20 ns, which differs from the starting, wild-type-like conformation.

The main change consists of a deformation of the strand segment around position 216, which in the mutant loses its $\beta$-sheet interaction with the adjacent segment 225-231. The backbone around ASP 216 protrudes towards the opposite side of the binding site, partially closing the enzyme speci-

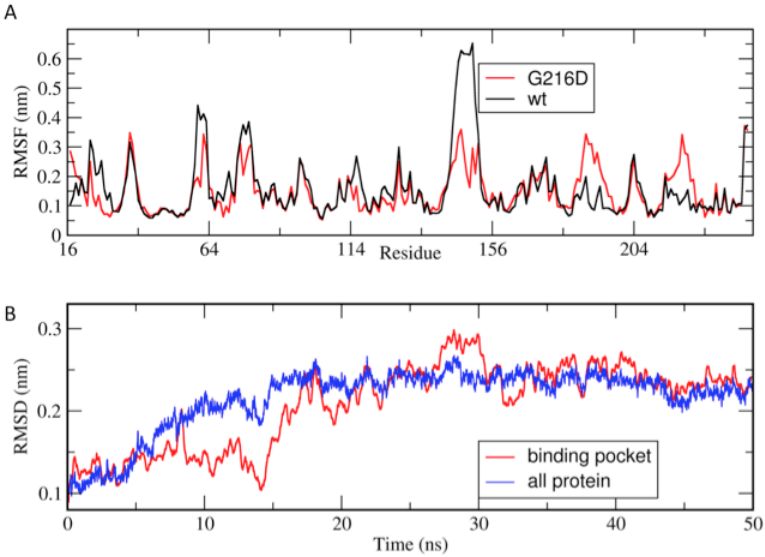


***Figure 5.3:*** *Panel A: graphic of RMS fluctuation of residues of G216D mutant and wild type during the MD simulation. RMSD profile of binding pocket and all protein of G216D mutant during the MD simulation is shown in panel B.*

ficity pocket for placement of arginine side-chain of substrate in the specificity pocket and hindering the access to ASP 189 (Figure 5.4).

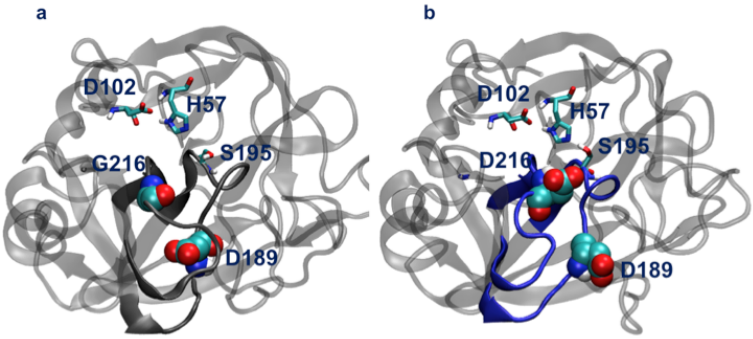


***Figure 5.4:*** *In this figure is shown a conformational change around the position 216. In G216D mutant the backbone around ASP 216 protrudes towards the opposite side of the binding site, partially closing the enzyme specificity pocket. Panel "a" wild type and panel "b" G216D mutant*

### 5.3.3 Docking simulations

To test the hypothesis of impairment of substrate recognition, we performed a flexible docking of the mutant structure with the PPACK inhibitor. The validation of the docking protocol was carried out by reproducing the X-ray complex of the wild type APC with PPACK ligand. The obtained RMSD value compared to X ray structure was 0,614 Ålower than the

threshold of 2.0 Åand indicating an accurate prediction of the ligand binding pose.

Docking simulation of Gly216Asp mutant with PPACK showed a remarkable change in binding mode compared to wild type (Figure 5.5a,b). In more detail, while the PPACK portion represented by Phe (D-F) and Pro (P) residues maintained an orientation similar to wild type, Arginine (R) side chain was deviated from the specificity pocket due to the steric hindrance of Asp216 that prevented the access to Asp189 of protein pocket (Figure 5.5c,d).

In addition, the incorrect positioning of the side chain of Arg shifted the ligand scissile peptide bond away from the O$\gamma$ of catalytic Ser195 by about 2 Åcompared to wild type. Therefore, in this configuration, the formation of the covalent bond between the C1 of ligand and the hydroxyl group of reactive Ser195 is prevented and the peptide bond hydrolysis cannot be started. We thus hypothesize that an impaired recognition of the enzyme substrate is responsible for the inhibition of enzymatic activity in Gly216Asp mutant.

## 5.4 Conclusion

Our molecular dynamics and docking simulations show that the mutation of Gly216 preserved the overall serine protease folding while impairing its enzymatic activity. These results are in agreement with the alpha tryptase and alpha-lytic protease reports (Mace and Agard, 1995; Marquardt et al., 2002). Structural superposition of APC x-ray structure with the molecular dynamics model shows that the RGD motif is structurally conserved after the mutational event, suggesting that the in-

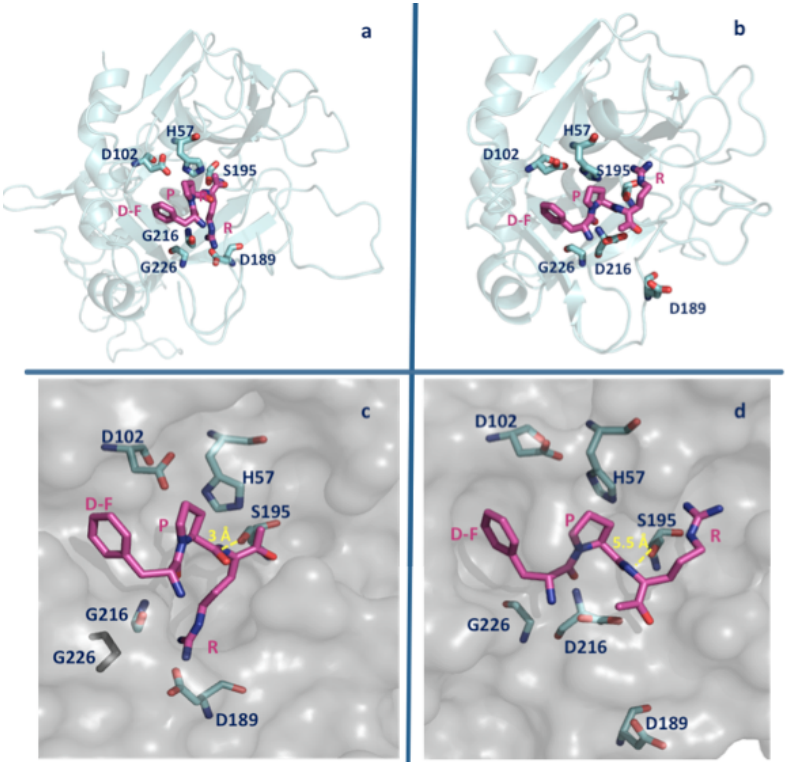


***Figure 5.5:*** *Docking simulation of wild type and G216D mutant with PPACK inhibitor. Panels a and c: docking pose of PPACK in wild type structure (ribbon representation and details of Connolly surface, respectively); panels b and d: same representation of docking pose in mutant. PPACK ligand and residues are shown in stick representation and colored by atom type.*

tegrin recognition may still occur even in the absence or reduction of protease function.

This observation is supported by the results obtained with thrombin (Papaconstantinou et al., 2005) showing that the RGD activity in retained also in the presence of structural rearrangements that impair the catalytic activity. The G216D mutant described here hints at the possibility of dissociating the serine protease activity of APC from its antiseptic function mediated by neutrophyl migration inhibition. It may, thus, be regarded as an useful tool to be evaluated for clinical applications where the anticoagulant activity can represent a threat of bleeding complications in patients.

# CHAPTER 6

# ANALYSIS OF THE EFFECTS OF POLLUTANTS

Pollutants, as we saw in chapter 1, can cause several adverse effects on human health. Adverse effects may occur to the respiratory and circulatory system but also to the endocrine system, the last effect is mainly due to endocrine disrupting chemicals (EDCs). The EDCs may act on the endocrine system and alter biological pathways, such as increasing the risks of cancer and disorders in metabolism, development and reproduction. It is therefore important to develop a tool for preliminary analysis in silico to investigate the possible effects of new pollutants on human health. In this context fits the work *Nuclear Receptor Database Evaluates the effects of the EDC on the Endocrine System* (manuscript in preparation) that lays the groundwork for a system of evaluation

of effects on endocrine system by EDCs. In the construction of this tool have been applied skills honed in previous works, in particular on the creation of 3D structures by homology techniques and evaluation of binding interactions by docking techniques. The realization of this work was made possible thanks to the configuration of a system of GRID computing that permit to reduce the computational time. At the end of the work it was possible to obtain a powerful tools to make a preliminary analysis of pollutants that allow to the identify the binding mode and evaluate the interaction energies between ligands and receptor.

## 6.1 Introduction

Many of the pollutants that are objects of deep environmental and toxicological studies are endocrine disrupting chemicals (EDCs). They derive both from natural and plant sources and also from synthetic chemicals designated for industrial applications, this last way is the more relevant. The natural EDCs are for example phytoestrogens and mycoestrogens, while synthetic chemicals are polychlorinated biphenyls, dioxins, plastics, plasticizers (bisphenol A), phthalates, pesticides (methoxychlor, chlorpyrifos, DDT) fungicides (vinclozolin), herbicides (atrazine), and antibacterials (triclosan). The exposure can not be reduced to zero and takes place through drinking water, breathing contaminated air, ingesting food. EDCs are structurally similar to many hormones and are able to exert their effect in different ways, for example bind a variety of nuclear receptors carrying out an agonist or antagonist action, also acting via multiple pathways such as membrane

receptors, the aryl hydrocarbon receptor, or the enzymatic machineries involved in hormone biosynthesismetabolism. Most of the toxicity studies of EDC are attributed to their interference with endocrine system mediated by Nuclear Hormone Receptors (NHR). NHRs regulate cognate gene networks involved in key physiological functions such as cell growth and differentiation, development, homeostasis, or metabolism. Each receptor has a non-redundant crucial role in these important biological processes (Laudet et al., 2004, 2006). NHRs are modular proteins composed of several domains, most notably an N-terminal domain which harbors a ligand-independent activation function (AF-1), a central DNA binding domain (DBD), and a C-terminal ligand binding domain (LBD) hosting a ligand-dependent transcriptional activation function (AF-2). The crystal structures of many NHR LBDs have been determined, revealing a conserved core of 12 $\alpha$-helices and a short two-stranded antiparallel $\beta$-sheet arranged into a three-layered sandwich fold. This arrangement generates a mostly hydrophobic cavity in the lower half of the domain which can accommodate the cognate ligand. The action of NR LBDs to activate transcription is controlled by the C-terminal helix 12 (AF-2 domain) (Bourguet et al., 2000; Li et al., 2003). The importance of helix 12 was became evident from the analysis of different crystal structures of the unliganded and ligand-bound LBDs of several NRs that suggest a mechanism of activation of nuclear receptors mediated by domain AF-2. In general after the binding of the ligand, occurs a conformational change that causes the repositioning of helix 11 and the subsequent shift of helix 12. Accordingly, the conformational change cause the proper shift of structural elements that permit to define

a correct NR surface for the interaction with transcriptional co-activators (Darimont et al., 1998). The importance of the AF-2 helix in regulating coactivator and corepressor is an important factor in the selection of the NR structure.

Based on the conservation of structural and functional NHR features and on the large structural and chemical diversity of compounds found in the environment, one can predict that all members of the NHR family are potential targets of EDCs. Thus, there is any endocrine system immune to these substances, due to common properties and the similarities of the nuclear receptors. The most studied interaction of EDCs is with the estrogen receptor, while studies on the role of nuclear receptors has been largely restricted to use of synthetic agonists. As previously mentioned the EDCs are xenobiotic or mixture that interfere with the endocrine system leading adverse effects on the health of an organism or its progeny, or of a subpopulation (DiVall, 2013; Buyukgebiz, 2012). Epidemiological and experimental studies suggest that EDCs may increase the risk of cancer, metabolic disorders, reproductive and developmental disorders In fact, epidemiological and in vitrovivo studies show alterations of the reproductive system, occurrence of neoplastic diseases and metabolic disorders. For example, a malfunction of the NR subfamilies of 1,2,5 cause alterations in lipid pathways (metabolism, storage, transport and disposal) that cause diseases associated with obesity, diabetes, and cardiovascular system difficulties and these diseases often appear to be correlated with exposure to EDCs (Chawla et al., 2001). The studies so far have focused primarily on Persistent Organic Pollutants (POPs), phthalates and BPA, but there is another class of EDCs strongly present in at-

mospheric pollutants, the Polycyclic aromatic hydrocarbons (PAHs). The environmental exposure to PAHs is shared by inhalation, ingestion and skin contact. The exposure levels in the environment are lower than those in the workplace, but smoking and diet can contribute substantially to the total PAH aspirated (Rooij et al., 1994) and also the inhalation of exhaust fumes in the areas urban is another component that affects the levels (Jongeneelen, 2001). The most present PAH in atmospheric pollutants is the benzo(a)pyrene (BaP) but the ability of the BaP to bind nuclear receptors, however, is still poorly analyzed. These evidences motivate the need to provide a system for the assessment of the interaction of various xenobiotics with nuclear receptors. Hence the need to implement a NRs database containing all possible structures useful to Molecular Docking simulations with any xenobiotics of interest (Shi and Wu, 2009). The three-dimensional protein structures were obtained from the Protein Data Bank (PDB) Database and with computational method such as homology modeling and fold recognition. The final result is a potent tool for preliminary in silico research applicable to old and newest primary or secondary pollutants and able to define the binding mode for each ligand compound, the binding energy and the possibility to act in place of the natural ligand.

## 6.2 Methods and Materials

In order to obtain a protocol able to assess the effects of EDCs on the endocrine system was implemented a database of 3D structures of the ligand binding domain of the nuclear receptors with homology modeling and fold recognition method.

A library of ligands was obtained considering co-crystalized structures, natural ligand and endocrin disruptors. Then were calculated the binding energies between receptors and ligands using docking techniques and, finally, the results were normalized to allow comparison.

### 6.2.1 Nuclear Receptor Database construction

The NRs database has been constructed mainly using Nuclear Receptors structures from Protein Data Bank (Rose et al., 2013) where there are 293 X-ray crystallographic structures of Ligand Binding Domain (LBD) corresponding to 29 members of the superfamily. A structure for each member of the superfamily was selected according to the following criteria:

i selected the structure in the agonist conformation;

ii selected the structure complexed with the natural ligand when it was available or that complexed with the ligand with agonist activity;

iii selected the structure without mutation and missing residues;

iv selected the structure with high-resolution.

We used homology modeling technique and fold recognition methods to model NR not available in PDB Database. For homology modeling technique the Ligand Binding Domain sequences of Nuclear Receptor protein were acquired from Swiss-Prot protein database (Jain et al., 2009). The sequence alignment BLASTP (Altschul et al., 1990) program from NCBI BLAST was used to search homologous sequences

of Homo Sapiens Nuclear Receptor against the PDB sequence database. Then ClustalW (Larkin et al., 2007) was utilized to align query sequence to template structure or structures, then the prediction of the 3D structure of query proteins was carried out by MODELLER 9v10 (Sali and Blundell, 1993) Five models were produced for each NR, each model was evaluated the stereochemical quality and stability using DOPE score Modeller, Q Mean (Benkert et al., 2009), Pro Q (Wallner and Elofsson, 2003) and Procheck programs (Laskowski et al., 1993). The I-Tasser (Zhang, 2008) program detects structure templates from the Protein Data Bank with fold recognition methods and the full-length structure models are constructed by reassembling structural fragments from threading templates using replica exchange Monte Carlo simulations. The models were minimized using the Sander module of Amber 12 Suite (Wang et al., 2001). For the minimization were performed 5000 cycles (2500 steepest descedent - 2500 conjugated gradient) using a cut-off of 12 Å. The library of ligands was built considering the co-crystallized ligands, the natural ligands and endocrine disruptors. The 3D structure of the ligands were obtained from the NR crystallized structures and the PubChem Databases (Bolton et al., 2008).

### 6.2.2 Docking set up

Docking simulations were performed with AutoDock 4.2.3 (Morris et al., 2009). The AutoDockTools (mgltools 1.5.4) was used to convert the ligand files to the pdbqt format by adding Gasteiger charges, checking polar hydrogens and assigning ligand flexibility. The ADT interface was employed to setup a grid box centred on the ligand binding domain. For most of

the receptors was carried out a grid of 90x90x90 points, while other receptors have required a grid of 76x88x66 points; so an affinity maps for all the atom types present, as well as an electrostatic map, were computed with a grid spacing of 0.375 Å. An automatic procedure, based on a Python script, was developed to execute the following ADT routines:

- *prepare_receptor* to add polar hydrogens and convert the protein PDB file in pdbqt;
- *prepare_gpf* generate the parameters file for AutoGrid
- *prepare_dpf* and for AutoDock.

The search was carried out with the Lamarckian Genetic Algorithm, the number of generations, energy evaluations, and docking runs were set to 50000, 25.000.000, and 150, respectively. Docking simulation was performed on a grid computing infrastructure (European Grid Infrastructure (EGI) (Kranzlmuller et al., 2010)), using an in-house developed software for computation management in EGI. By using a pilot job strategy, the software allowed easy job submission, automatic detection and management of Grid failures, job scheduling with nearto-constant throughput, and other advanced features allowing to carry on the large computations required reliably and with highly predictable completion times. Each docking simulation returns a set of clusters ranked by the binding energy. The selection of a final conformation was performed through a homemade program that selects the most populated cluster in a range of $0.5 kcal/mol$ compared to the energy minimum.

### 6.2.3 Statistical Analysis

The docking simulation of ligands against the receptors were performed using the previous protocol. The results are receptor and ligand dependent, so it is impossible compare the energy of different simulations therefore a normalization (Lauro et al., 2012) was performed on the predicted binding energies, using the Equation 6.1.

$$E_{DN} = \frac{E_D}{(A_{ER} + A_{EL})/2} \tag{6.1}$$

where $E_{DN}$ is the normalized value associated to each receptor-ligand complex, $E_D$ is the value of predicted binding energy obtained from the docking calculation (kcal/mol), $A_{ER}$ and $A_{EL}$ are the average binding energy,respectively, each receptor (on different ligands, kcal/mol) and each ligand (on the various receptors, kcal/mol). This mathematical manipulation causes the loss of the original significance of the binding energy as a value for the prediction of activity of a given receptor-ligand complex but can be used to generate a ranking in which the best values represent a best interaction between a ligand and a nuclear receptor. Moreover, taking into account the average trends in Equation 6.1. the selection of false positive results can be avoided. The average trends due to $A_{ER}$ and $A_{EL}$ parameters permit also to exclude eventual false positive results.

## 6.3 Result and Discussion

### 6.3.1 Nuclear Receptor Database

The database of nuclear receptors has been implemented thanks to the crystallographic structures and techniques of ho-

mology modeling and fold recognition. According to the criteria explained in the session 6.2.1 we selected 29 crystal structures, reported in Table 6.1. As mentioned in the introduction (6.1) the 12 helix of the nuclear receptor is important for the activity of the receptor, so the receptors must be selected in the same conformation to permit the studies of interactions with ligands. All structures were then selected in the agonist conformation. Regarding the receptors bound to ligands have been selected 11 structures related to their natural ligand and 10 structures linked to another ligand with agonist function. The structures of the 8 orphan receptors were carried out considering the completeness of the ligand binding domain and the X-Ray resolution.

Receptors not available in PDB has been obtained by modeling them with computational techniques. We used homology modeling technique to model 15 nuclear receptors. For 12 receptors were identified as homologous proteins from PDB that showed a sequence identity including between 39% to 99%; while for three receptors (NR2C1, NR2C2 and NR2E1) were identified more templates because a single template does not contain region of similarity to the entire sequence. For these receptors, the identity of the sequence was between 31% to 37%. Finally NR3B1 and NR6A1 were modeled with fold recognition methods.

The last two receptors DAX-1 and SHP belonging to the group NR0B weren't modeled because they are as substantially different from other nuclear receptors in terms of both structure and function. Infacts the search with BLASTP reported an identity of sequence 25% lower and therefore not relevant. While I-Tasser has not been able to identify significant pro-

***Table 6.1:*** *Crystallized structures selected from the PDB database, and ligands co-crystalizzed to them*

| **Nuclear Receptors** | **NRNC Symbol** | **PDB CODE** | **Natural Ligand** |
|---|---|---|---|
| TR $\alpha$ | NR1A1 | 2H79 | Yes (thyroid hormone T3) |
| TR $\beta$ | NR1A2 | 2J4A | No |
| RAR $\alpha$ | NR1B1 | 3A9E | retinoic acid |
| RAR $\beta$ | NR1B2 | 4DM6 | No retinoic acid |
| RAR $\gamma$ | NR1B3 | 2LBD | Yes (retinoic acid ) |
| PPAR $\alpha$ | NR1C1 | 2P54 | No |
| PPAR $\beta/\delta$ | NR1C2 | 3GWX | Yes (fatty acids) |
| PPAR $\gamma$ | NR1C3 | 3ADW | Yes (fatty acids) |
| Rev-ErbA $\beta$ | NR1D2 | 3CQV | Orphan |
| ROR $\alpha$ | NR1F1 | 1N83 | Orphan |
| ROR $\gamma$ | NR1F3 | 3L0L | Orphan |
| LXR $\alpha$ | NR1H3 | 3IPQ | No |
| LXR $\beta$ | NR1H2 | 1UPV | No |
| FXR | NR1H4 | 3OLF | No |
| VDR | NR1I1 | 1IE9 | Yes (vitamin D3) |
| PXR | NR1I2 | 1NRL | No |
| CAR | NR1I3 | 1XVP | No |
| HNF4 $\alpha$ | NR2A1 | 3FS1 | Orphan |
| HNF4 $\gamma$ | NR2A2 | 1LV2 | Orphan |
| RXR $\alpha$ | NR2B1 | 1G5Y | Yes (retinoic acid) |
| RXR $\beta$ | NR2B2 | 1UHL | No |
| ER $\alpha$ | NR3A1 | 1G50 | Yes (estradiol) |
| ERR $\gamma$ | NR3B3 | 2GPU | Orphan |
| GR | NR3C1 | 3BQD | No |
| MR | NR3C2 | 2A3I | Yes (corticosterone) |
| PR | NR3C3 | 1A28 | Yes (progesterone) |
| AR | NR3C4 | 2AM9 | Yes (testosterone) |
| SF1 | NR5A1 | 1ZDT | Orphan |
| LRH-1 | NR5A2 | 3PLZ | Orphan |

***Table 6.2:*** *Structures of NR modeled with homology modeling technique and fold recognition methods.*

| **Nuclear Receptors** | **NRNC Symbol** | **PDB CODE** | **% of identity** |
|---|---|---|---|
| *Homology Modeling* | | | |
| Rev-ErbA$\alpha$ | NR1D1 | 1NQ7 | 41 |
| ROR $\beta$ | NR1F2 | 1NQ7 | 99 |
| RXR $\gamma$ | NR2B3 | 1MV9 | 90 |
| TR2 | NR2C1 | 1RDT | 32 |
| | | 1Z5X | 34 |
| TR4 | NR2C2 | 3E94 | 33 |
| | | 4IQR | 31 |
| TLX | NR2E1 | 1MV9 | 37 |
| | | 1UOM | 31 |
| PNR | NR2E3 | 1XLS | 39 |
| COUP-TFI | NR2F1 | 1RDT | 45 |
| COUP-TFII | NR2F2 | 3UVV | 45 |
| EAR-2 | NR2F6 | 3DZU | 46 |
| ER $\beta$ | NR3A2 | 1G50 | 57 |
| ERR$\beta$ | NR3B2 | 1KV6 | 79 |
| NGFIB | NR4A1 | 1PDU | 66 |
| NURR1 | NR4A2 | 1OVL | 98 |
| NOR1 | NR4A3 | 1OVL | 65 |
| *Fold Recognition* | | | |
| ERR $\alpha$ | NR3B1 | 3DZY | |
| | | 4IQR | |
| GCNG | NR6A1 | 3DZY | |

teins because part of the ligand binding domain remained not moldable Due to computational techniques have been modeled structures of 17 nuclear receptors (Table 6.2). As highlighted in the introduction (6.1), a important class of EDCs are PAHs, in particular BaP. So it is important to assess the interaction of BaP with NHRs and to do this is needed to consider that several studies show an interaction between BaP and aryl hydrocarbon receptor (AHR). Consequently, the interaction with AHR must be taken into account for the evaluation of affinity with NHRs. The X-ray structure of the AHR is not present in the PDB database, so it was created to homologia using as a template structure with 27% identity (PDB Code: 4F3L). In conclusion, the database consists of 47 three-dimensional structures of receptors. At the same time has been created the library of ligands, containing 16 crystallographic ligand, 18 natural ligand and 10 EDCs.

### 6.3.2 Docking and Statistical Analysis

The docking protocol previously described was applied to all of the receptor-ligand pairs. The first step is validating the protocol, so were made re-docking simulations of the crystal structures with natural ligands in order to validate the methodology applied.

The redocking of all the complexes with the natural ligand showed the same behavior: correct orientation in the binding pocket and H-bonds comparable with those reported in the X-ray structure.

Subsequently, the protocol was applied to all ligand-receptor pairs. Considering the amount of calculations required simulations were carried out on GRID Computing Infrastructure,

allowing the lowering of computational time. A single docking simulation takes approximately 7 hours of computing time, so with a single CPU takes about 14476 hours ($\sim$ 20 months) while on GRID infrastructure are sufficient $\sim$ 63 hours.

Using this protocol a database of 47 receptor was complexed with a library of 44 ligands and the results collected in a matrix. This predicted binding energy aren't comparable because the Autodock Function Energy have ligand and receptor bias, so the matrix was been normalized with Equation 6.1. The normalized matrix can be analyzed by observing different factors:

- Which ligand interacts more strongly with a specific receptor
- Which receptor will preferably be linked to a specific ligand
- Comparison of the binding capacity of the ligands with respect to the natural ligand

For example considering the ligand Benzo(a)pyrene (BaP) and its derivative 2-hydroxybenzo(a)pyrene (2-OH BaP) is possible to observe how they has a good ability to bond with the majority of nuclear receptors where it is found that the value of interaction appears to be always above the average value of the matrix.

The ability of interaction of these two ligands is observable also analyzing the poses of bond. For example, as shown in Figure 6.1 relative to the Estrogen Receptor $\alpha$, both BaP and 2-OH BaP are positioned in the binding pocket in a manner similar to the natural ligand (EST) and with comparable energy.

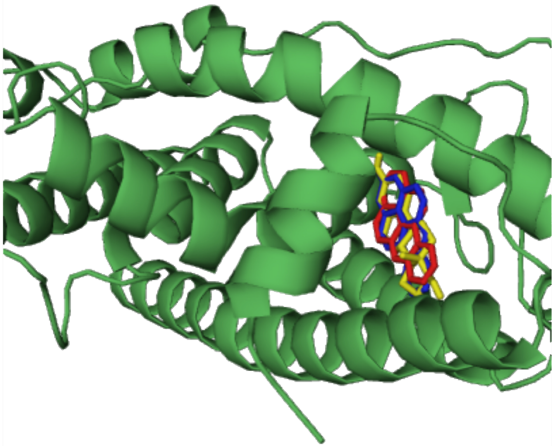

***Figure 6.1:*** *In figure is represented the ERα receptor structure and are shown the binding pose for EST (yellow),BaP (red) and 2-OH BaP (blue). The energy are, respectively, -10.37 kcal/mol (1.35), -9.69 kcal/mol (1.23) and -10.03 kcal/mol (1.27)*

Finally, the last analysis consists of a comparison against the binding energy of the natural ligands. This value indicates the ability of a ligand to unseat the natural ligand and act as it. In particular, observing the BaP and 2-OH BaP for some receptor their binding affinity is similar or superior compared to the natural ligand affinity (Table 6.3).

## 6.4 Conclusion

In this work was been created a database of 3D structures of nuclear hormone receptors that includes: X -ray structures

***Table 6.3:*** *Comparison of normalized binding energy for BaP and 2-OH BaP against natural ligands*

| Receptor | Natural Ligand | BaP | 2-OHBaP |
|---|---|---|---|
| PPAR$\alpha$ (NR1C1) | 0.90 | 1.05 | 1.10 |
| PPAR$\beta$ (NR1C2) | 0.86 | 1.01 | 1.00 |
| LXR$\alpha$ (NR1H3) | 0.92 | 1.07 | 1.07 |
| FXR (NR1H4) | 0.80 | 1.01 | 1.00 |

from the PDB database and computational models from homology modeling and fold recognition. The database also includes the 3D structure of the AhR receptor important for its interactions with benzo(a)pyrene. Parallel to the database has been created a library of ligands, really important is the presence of natural ligands, which are used as indicators of interaction with the receptors. The confront of an xenobiotic-receptor interaction against the natural ligands-receptor complex is a powerful tools to understand the possibility of a xenobiotic to act in contrast to the natural ligand. This tools is been applied as first analysis tool for the evaluation of the effects of EDCs on the endocrine system caused by the interaction of these with the nuclear hormone receptor superfamily. In particular, it was observed that BaP interacts with certain receptors with greater affinity than their natural receptors allowing to presume its interference in the metabolic pathway governed by the latters. In particular the deregulation of these receptors may constitute a factor for attracting risk for the development of important metabolic diseases such as metabolic syndrome, obesity and diabetes mellitus type 2.

# CHAPTER 7

# CONCLUSIONS

In modern society, one of the most important problems is the air pollution, as there is a correlation between the level of pollution and damage to the environment and human health. Particulate pollution is the most important and significant liable for damage to human health among the different types of pollution (solid, liquid or gaseous).

There are several models for the prediction of concentration and chemical composition of particulate matter, while only few models have been published in the field of particulate matter effects on human health and enviromental. This is due to the fact that PM is a very heterogeneous class of materials, not only in terms of their chemical composition, but also in terms of size, shape, agglomeration state and surface reactivity. So it is important to develope new computational models to predict these effects on enviromental and human health.

In the field of environmental effects play a vital role the process of corrosion of materials. The PM is able to influence the corrosion process through different activities, this is made possible by a presence of substances able to change the speed of corrosion and to participate in the reactions of galvanic corrosion. Acidification of soils can lead to release of toxic elements such as aluminum , resulting in serious damage to the plants and various forms of aquatic life. In additional there are direct effects on vegetation in function of the acid and oxidizing action of the particles, which leads to damage to the plant tissues. The erosion of the materials is mainly due to rain , sulfur depositions , nitric acid and intake of acidity. The atmospheric particulate causes the tarnish of the materials. One of the key factors in the activity of the corrosive atmospheric particulate matter is the relative humidity. A study on the influence of the RH has been carried out in order to evaluate the impact of the corrosivity in indoor environments. In particular the study on a Data Center has led to the development of a protocol to define the optimal DFC operating cycle to preserve the circuit elements of Printed Circuit Boards and at the same time reduce the energy consumption operated by the Data Center. This purpuse was achieved through the determination of the most reliable thermodynamic limits (especially moisture) based on in-situ measured aerosol properties. This protocol can be applied to any DC to estimate economic and environmetal costs in feasibility studies; this is possible because the aerosol properties (in particular chemical composition, DRH and acidity) and meteorological parameters were investigated using reliable and shared methods, characterized by reasonable costs. The case study reported in Chapter 3 suggests the

practicability to use a DFC. In particolar it suggests the use of a specific filtering system and a best thermal cycle to obtain an energy saving of 81% compared to traditional AC cooling systems and at the same time preserve the circuit elements.

In the field of human health effects,as shown by the literature data, the majority of the information are derived from epidemiological studies, or to a lesser extent, on experimental studies in vivo or in vitro. So for economic and time reasons, in parallel to these studies, is important to develop computational models to evaluate the molecular interactions that occur between PM components and human receptors. These interactions can be an important element to underline the mechanism of action that leading to effects on human health and to understand the possibility effects of new pollutants.

In this PhD thesis, several computational methods have been used:

- homology modeling and fold recognition in order to obtain 3D structures of studied proteins,
- molecular docking to evaluate the binding mode and the binding affinity of the complexes,
- molecular dynamic to evaluate the stability of the complexes and the identification of key residues interacting molecular

To best use the methods described above it was necessary to configure new computing infrastructures that best lend themselves to the type of computations to be performed. In particular, in order to perform long molecular dynamics was necessary to prepare an infrastructure of GPU computing that

thanks to their superior performance allows to reduce the computational time compared to the standard simulations performed on clustering computing. In addition, it becomes possible to lengthen the simulated time to better understand the binding mechanisms that occur and to better assess the stability of the different bonds. It was necessary to prepare also the use of grid computing infrastructure to carry out a greater number of concurrent simulations and thus drastically reduce the computation time for the docking simulations.

In Chapter 4 has been highlighted the importance of the specificity and selectivity of proteins. In particular the lack of X-ray has made fundamental the realization of a in silico protocol to gain a better understanding of the enzyme-inhibitor interactions. This protocol permit to screening a ligand library and underlines the key bonds that occur in the complex. In fact, thanks to this protocol a predictive 3D PDE11 model has been. This protocol permits to obtain useful information for the design of new potent and selective compounds. The long MD simulation has allowed to identify the fundamentals residues involved in the ligand-enzyme binding process, and this information can be use in future works to design and synthesis of new and more potent selective PDE11 inhibitors.

In Chapter 5 has been underlined the importance of a infrastructure with high performance and has been designed a protocol for computational study of the functional activity of protein C. This protocol involved the simulation of various docking simulation to better understand the protein interaction. Moreover has been developed a new scoring function that included biological information of the interaction of the protein in addition to the energies of docking to better rank-

ing the results of docking. The results permit to observe that integrin recognition may still occur even in the absence or reduction of protease function. This protocol can be an useful tool to evaluated the protein functionality after mutagenesis, in particolar the protein C mutated can be used for his antisepsi activity in patients where the anticoagulant activity can represents a threat of bleeding complications.

In the last chapter (Chapter 6) has been exposed a tool for preliminary analysis in silico to investigate the effects of pollutants on human health. The development of this protocol has required the application of all the skills acquired in the other Chapters (4 e 5) in particular the capability to model the 3D structures and performe large scale docking simulations. The realized database can be used to testing new pollutants and compare their activity against the natural ligand activity. In facts, this tools has been applied as first analysis tool to evaluate the effects of EDCs on the endocrine system caused by the interaction of these ligands with the nuclear hormone receptor superfamily .

Through all these works it was possible to achieve the computational models to better understand the effects of atmospheric particulates on the environment and human health. In particular different protocols has been developed:

1. a protocol to evaluate the effects of PM on circuit elements in function of DRH, that can be use to better configurate Data Center to reduce the energy required for the cooling system and at the same time preserve the Printed Circuit Boards

2. a protocol to underline the key residues of interaction

with the aim of design new potent and selective compounds,

3. a protocol to highlight protein functionality,

4. a protocol in order to understand the effects of new pollutants on the endocrine system due to a higher binding affinity for receptors

# BIBLIOGRAPHY


Altschul, S., Gish, W., Miller, W., Myers, E., and Lipman, D. (1990). Basic local alignment search tool. *J. Mol. Biol.*, 215:403–410.

Bairoch, A. and Apweiler, R. (2000). The swiss-prot protein sequence database and its supplement trembl in 2000. *T. Nucleic Acids Res*, 28:45–48.

Bassett, M. and Seinfeld, J. H. (1983). Atmospheric equilibrium model of sulphate and nitrate aerosols. *Atmos. Environ.*, 17:2237–2252.

Behndig, A., Mudway, I., Brown, J., Stenfors, N., Helleday, R., and et al (2006). Airway antioxidant and inflammatory responses to diesel exhaust exposure in healthy humans. *Eur Resp J*, 27:359–365.

Benkert, P., Kunzli, M., and T., S. (2009). Qmean server for protein model quality estimation. *Nucleic Acids Res.*, 37.

Berendsen, H. J. C., Postma, J. P. M., Van Gunsteren, W. F., and Hermans, J. (1081). Interaction models for water in relation to protein hydration. *Intermolecular forces*, pages 331–334.

Berman, H., Westbrook, J., Feng, Z., Gilliland, G., Beth, T., Weissig, H., Shindyalov, I., and Bourne, P. (2000). The protein data bank. *Nucleic Acids Res*, 28:235–242.

Bolton, E., Y, W., Thiessen, P., and Bryant, S. (2008). Pubchem: Integrated platform of small molecules and biological activities. *American Chemical Society*.

Bond, T., Doherty, S., Fahey, D., Forster, P., Berntsen, T., Deangelo, B., Flanner, M., Ghan, S., Karcher, B., Koch, D., Kinne, S., Kondo, Y., and Quinn, P. (2013). Bounding the role of black carbon in the climate system: A scientific assessment. *Journal of Geophysical Research: Atmospheres*, 118:1–173.

Bourguet, W., Germain, P., and Gronemeyer, H. (2000). Nuclear receptor ligand-binding domains: three-dimensional structures, molecular interactions and pharmacological implications. *Trends Pharmacol Sci*, 21:381–388.

Brook, R., Rajagopalan, S., Pope, A., Brook, J., Bhatnagar, A., Diez-Roux, A., and et al (2010). Particulate matter air pollution and cardiovascular disease: an update to the scientific statement from the american heart association. *Circulation*, 121:2331–2378.

Buyukgebiz, T. U. A. (2012). Fetal and neonatal endocrine disruptors. *J Clin Res Pediatr Endocrinol*, 4(2):51–60.

Cape, J., Coyle, M., and Dumitrean, P. (2012). The atmospheric lifetime of black carbon. *Atmopheric Environment*, 59:256–263.

Carbone, C., Decesari, S., Mircea, M., Giulianelli, L., Finessi, E., Rinaldi, M., Fuzzi, S., Marinoni, A., Duchi, R., Perrino, C., Sargolini, T., Varde, M., Sprovieri, F., Gobbi, G. P., Angelini, F., and Facchini, M. C. (2010). Size-resolved aerosol chemical composition over the italian peninsula during typical summer and winter conditions. *Atmospheric Environment*, 44(39):5269–5278.

Card, G., England, B., Suzuki, Y., Fong, D., Powell, B., Lee, B., and Luu, C. e. a. (2004). Structural basis for the activity of drugs that inhibit phosphodiesterases. *Structure*, 12:2233–2247.

Ceyhan, O., Birsoy, K., and Hoffman, C. (155-163). Identification of biologically active pde11-selective inhibitors using a yeast-based high-throughput screen. *Chem Biol*, 19:155–163.

Chakrabarty, R., Garro, M., Wilcox, E., and Moosmuller, H. (2012). Strong radiative heating due to wintertime black carbon aerosols in the brahmaputra river valley. *Geophysical Research Letters*, 39(9).

Chaudhury, S., Berrondo, M., Weitzner, B. D., Muthu, P., Bergman, H., and Gray, J. J. (2011). Benchmarking and analysis of protein docking performance in rosettadock v3.2. *PLoS One*, 6.

Chawla, A., Repa, J., Evans, R., and Mangelsdorf, D. (2001). Nuclear receptors and lipid physiology: opening the x-files. *Science*, 294:1866–1870.

Chen, L. and Nadziejko, C. (2005). Effects of subchronic exposures to concentrated ambient particles (caps) in mice. v. caps exacer- bate aortic plaque development in hyperlipidemic mice. *Inhal Toxicol*, 17(4-5):217–224.

Chuang, K., Chan, C., Su, T., Lee, C., and Tang, C. (2007). The effect of urban air pollution on inflammation, oxidative stress, coagulation, and autonomic dysfunction in young adults. *Am J Respir Crit Care Med*, 176(2):370–376.

Comeau, S. R., Gatchell, D. W., Vajda, S., and Camacho, C. J. (2004). Cluspro: An automated docking and discrimination method for the prediction of protein complexes. *Bioinformatics*, 20:45–50.

Cornell, W., Bayly, C., Gould, I., Merz, K., Ferguson, D., Spellmeyer, D., Fox, T., Caldwell, J., and Kollman, P. (1995). A second generation force field for the simulation of proteins, nucleic acids and organic molecules. *J Am Chem Soc*, 117:5179–5196.

Corrigan, C. E., Roberts, G. C., Ramana, M. V., Kim, D., and Ramanathan, V. (2008). Capturing vertical profiles of aerosols and black carbon over the indian ocean using autonomous unmanned aerial vehicles. *Atmospheric Chemistry and Physics*, 8(3):737–747.

Daher, N., Ruprecht, A., Invernizzi, G., De Marco, C., Miller-Schulze, J., Bae Heo, J., Shafer, M. M., Shelton, B. R., Schauer, J. J., and Sioutas, C. (2012). Characterization, sources and redox activity of fine and coarse particulate matter in milan, italy. *Atmos. Environ.*, 49:130–141.

Darimont, B. D., Wagner, R. L., and Yamamoto., K. R. (1998). Structure and specificity of nuclear receptor-coactivator interactions. *Genes Dev.*, 12:3343–3356.

Di Nicolantonio, W., Cacciari, A., Petritoli, A., Carnevale, C., Pisoni, E., Volta, M., Stocchi, P., Curci, G., Bolzacchini, E., Ferrero, L., Ananasso, C., and Tomasi, C. (2009). Modis and omi satellite observations supporting air quality monitoring. *Radiat. Prot. Dosim.*

Diez-Roux, A., Auchincloss, A., Astor, B., Barr, R., Cushman, M., Dvonch, T., Jacobs, D., Kaufman, J., Lin, X., and Samson, P. (2006). Recent exposure to particulate matter and c-reactiveprotein concentration in the multi-ethnic study of atherosclerosis. *Am J Epidemiol*, 164(5):437–448.

DiVall, S. (2013). The influence of endocrine disruptors on growth and development of children. the influence of endocrine disruptors on growth and development of children. the influence of endocrine disruptors on growth and development of children. the influence of endocrine disruptors on growth and development of children. *Curr Opin Endocrinol Diabetes Obes*, 20(1):50–55.

Dockery, D. W., Pope, C. A., Xu, X., Spengler, J. D., Ware, J. H., Fay, M. E., Jr., B. G. F., and Speizer, F. E. (1993). An association between air pollution and mortality in six u.s. cities. *N Engl J Med*, 329:1753–1759.

Driscoll, K., Lindenschmidt, R., Maurer, J., Higgins, J., and Ridder, G. (1990). Pulmonary response to silica or titanium dioxide: inflammatory cells, alveolar macrophage-derived cytokines, and histopathology. *Am J Respir Cell Mol Biol*, 2(4):381–390.

Esmon, C. T. (2006). Inflammation and the activated protein c anticoagulant pathway. *Seminars in Thrombosis and Hemostasis*, 32:49–60.

Fawcett, L., Baxendale, R., Stacey, P. amd McGrouther, C., Harrow, I., Soderling, S., Hetman, J., Beavo, J., and Phillips, S. (2000). Molecular cloning and characterization of a distinct human phosphodiesterase gene family: Pde11a. *Proc Natl Acad Sci*, 97:3702–3707.

Fechteler, T., Dengler, U., and Schomberg, D. (1995). Prediction of protein three-dimensional structures in insertion and deletion regions: a procedure for searching data bases of representative protein fragments using geometric scoring criteria. *J Mol Biol*, 253:114–131.

Ferrero, L., Cappelletti, D., Moroni, B., Sangiorgi, G., Perrone, M., Crocchianti, S., and Bolzacchini, E. (2012). Wintertime aerosol dynamics and chemical composition across the mixing layer over basin valleys. *Atmospheric Environment*, 56(0):143 – 153.

Ferrero, L., Riccio, A., Perrone, M. G., Sangiorgi, G., Ferrini, B. S., and Bolzacchini, E. (2011b). Mixing height determination by tethered balloon-based particle soundings and modeling simulations. *Atmospheric Research*, 102(1-2):145–156.

Ferrero, L., Sangiorgi, G., Ferrini, B. S., Perrone, M. G., Moscatelli, M., D'Angelo, L., Rovelli, G., Ariatta, A., Truccolo, R., and Bolzacchini, E. (2013). Aerosol corrosion prevention and energy-saving strategies in the design of green data centers. *Environmental science & technology*, 47(8):3856–3864.

Forbes, L., Patel, M., Rudnicka, A., Cook, D., Bush, T., Stedman, J., Whincup, P., Strachan, D., and Anderson, R. (2009). Chronic exposure to outdoor air pollution and markers of systemic inflammation. *Epidemiology*, 20(2):245–253.

Francis, S., Turko, I., and Corbin, J. (2001). Cyclic nucleotide phosphodiesterases: relating structure and function. *Prog Nucleic Acid Res Mol Biol*, 65:1–52.

Hansen, J. and Lacis, A. (1990). Sun and dust versus greenhouse gases: An assessment of their relative roles in global climate change. *Nature*, 346:713–719.

Hetman, M., Robas, N., Baxendale, R., Fidock, M., Phillips, S., Soderling, S., and Beavo, J. (2000). Cloning and characterization of two splice variants of human phosphodiesterase 11a. *Proc Natl Acad Sci*, 97:12891–12895.

Hoffmann, B., Moebus, S., Dragano, N., Stang, A., Mohlenkamp, S., Schmermund, A., Memmesheimer, M., Brocker-Preuss, M., Mann, K., Erbel, R., and Jockel, K. (2009). Chronic residential exposure to particulate matter air pollution and systemic inflammatory markers. *Environ Health Perspect.*, 117(8):1302–1310.

Hogg, J., Chu, F., Utokaparch, S., Woods, R., Elliott, W., and et al (2004). The nature of small-airway obstruction in chronic obstructive pulmonary disease. *NEJM*, 350(26):2645–2653.

Hueglin, C., Gehrig, R., Baltensperger, U., Gyselc, M., and Monnd, C. nad Vonmonta, H. (2005). Chemical characterisation of pm2.5, pm10 and coarse particles at urban, near-city and rural sites in switzerland. *Atmos. Environ.*, 38:3305–3318.

Jacobson, M., Tabazadeh, A., and Turco, R. (1996). Simulating equilibrium within aerosols and nonequilibrium between gases and aerosols. *J. Geophys. Res.*, 101:9079–9091.

Jain, E., Bairoch, A., Duvaud, S., Phan, I., Redaschi, N., Suzek, B., Martin, M., McGarvey, P., and Gasteiger, E. J. (2009). Infrastructure for the life sciences:

design and implementation of the uniprot website. *BMC Bioinformatics*, 10(136).

Jakalian, A., Jack, D., and Bayly, C. (2002). Fast, efficient generation of high-quality atomic charges. am1-bcc model: Ii. parameterization and validation. *J Comput Chem*, 23:1623–1641.

Jongeneelen, F. (2001). Benchmark guideline for urinary 1-hydroxypyrene as biomarker of occupational exposure to polycyclic aromatic hydrocarbons. *Ann. Occup. Hyg.*, 45:3–13.

Kanakidou, M., Seinfeld, J., Pandis, S., Barnes, I., Dentener, F., Facchini, M., Dingener, R. V., Ervens, B., Nenes, A. ., Nielsen, C., Swietlicki, E., Putaud, J., Balkanski, Y., Fuzzi, S., Horth, J., Moortgat, G., Winterhaltor, R., Myhre, C., Tsigaridis, K., Vignati, E., Stephanou, E., and Wilson, J. (2005). Organic aerosol and global climate modeling: a review. *Atmos. Chem. Phys*, 5(1053-1123).

Kim, Y., Seinfeld, J., and Saxena, P. (1993). Atmospheric gas-aerosol equilibrium, i, thermodynamic model. *Aerosol Sci. Technol.*, 19:157–181.

Kinami, N. (2007). Environmental pollution and impact to public health, a pilot study report in cooperation with the united nations environment programme (unep), nairobi, kenya. Technical report.

Kozakov, D., Hall, D. R., Beglov, D., Brenke, R., Comeau, S. R., Shen, Y., and Vajda, S. (2010). Achieving reliability and high accuracy in automated protein docking: Cluspro, piper, sdu, and stability analysis in capri rounds 13-19. *Proteins: Structure, Function, and Bioinformatics*, 78:3124–3130.

Kranzlmuller, D., Lucas, J. M., and Oster, P. (2010). The european grid initiative (egi). *Remote Instrumentation and Virtual Laboratories*, pages 61–66.

Kumar, N., Lurmann, F., and Chico, T. (1998). Modeling the effects of emission changes on pm2.5 using the uam-aero model in the south coast air basin. (737-747).

Larkin, M., Blackshields, G., Brown, N., Chenna, R., McGettigan, P., McWilliam, H., Valentin, F., Wallace, I., Wilm, A., Lopez, R., Thompson, J., Gibson, T., and Higgins, D. (2007). Clustalw and clustalx version 2. *Bioinformatics*, 23:2947–2948.

Laskowski, R. A., MacArthur, M. W., Moss, D. S., and Thornton, J. M. (1993). Procheck - a program to check the stereochemical quality of protein structures. *J. App. Cryst*, 26:283–191.

Laudet, V., Germain, P., Staels, B., Dacquet, C., and Spedding, M. (2006). Overview of nomenclature of nuclear receptors. *Pharmacol Rev*, 58:685–704.

Laudet, V., Gronemeyer, H., and JA, J. G. (2004). Principles for modulation of the nuclear receptor superfamily. *Nat Rev Drug Discov*, 3:950–964.

Lauro, G., Masullo, M., Piacente, S., Riccio, R., and Bifulco, G. (2012). Inverse virtual screening allows the discovery of the biological activity of natural compounds. *Bioorganic & Medicinal Chemistry*, 20(11):3596 – 3602.

Li, Y., Lambert, M., and Xu, H. (2003). Activation of nuclear receptors: a perspective from structural genomics. *Structure*, 11:741–746.

Li, Z., Cai, Y., Cheng, Y., Lu, X., Shao, Y., Li, X., Liu, M., Liu, P., and Luo, H. (2013). Identification of novel phosphodiesterase-4d inhibitors pre-screened by molecular dynamics-augmented modeling and validated by bioassay. *J Chem Inf Model*, 53:972–981.

Lobnig, R. E., Frankenthal, R. P., Siconolfi, D. J., Sinclair, J. D., and Stratmann, M. (1994). Mechanism of atmospheric corrosion of copper in the presence of submicron ammonium sulfate particles at 300 and 373 k. *J. Electrochem. Soc.*, 141(11):2935–2941.

M., C. and J., B. (2007). Biochemistry and physiology of cyclic nucleotide phosphodiesterases: essential components in cyclic nucleotide signaling. *Annu Rev Biochem*, 20:481–511.

M., L. (1992). Accurate modeling of protein conformation by automatic segment matching. *J Mol Biol*, 226:507–533.

Mace, J. E. and Agard, D. A. (1995). Kinetic and structural characterization of mutations of glycine 216 in alphalytic protease: A new target for engineering substrate specificity. *Journal of Molecular Biology*, 4:720–736.

Maletto, A., McKendry, I., and Strawbridge, K. (2003). Profiles of particulate matter size distributions using a balloon-borne lightweight aerosol spectrometer in the planetary boundary layer. *Atmospheric Environment*, 37:661–670.

Marquardt, U., Zettl, F., Huber, R., Bode, W., and Sommerhoff, C. (2002). The crystal structure of human alpha1-tryptase reveals a blocked substrate-binding region. *Journal of Molecular Biology*, 321:491–502.

Martin, S. (2000). Phase transitions of aqueous atmospheric particles. *Chem.Rev.*, 100(9):3403–3453.

McMeeking, G., Hamburger, T., Liu, D., Flynn, M., Morgan, W., Northway, M., Highwood, E., Krejci, R., Allan, J., Minikin, A., and Coe, H. (2010). Black carbon measurements in the boundary layer over western and northern europe. *Atmospheric Chemistry and Physics*, 10(19):9393–9414.

Meng, Z., Dabdub, D., and Seinfeld, J. (1997). Chemical coupling between atmospheric ozone and particulate matter. *Science*, 277:116–119.

Miller, C. and Yan, C. (2010). Targeting cyclic nucleotide phosphodiesterase in the heart: therapeutic implications. *J Cardiovasc Transl Res*, 5:507–515.

Miller, K., Siscovick, D., Sheppard, L., Shepherd, K., Sullivan, J., and et al (2007). Long-term exposure to air pollution and incidence of cardiovascular events in women. *NEJM*, 356:447–458.

Moro, S., Deflorian, F., Bacilieri, M., and G., S. (2006). Ligand-based homology modeling as attractive tool to inspect gpcr structural plasticity. *L Curr Pharm Des*, 12:2175–2185.

Morris, G. M., Huey, R., Lindstrom, W., Sanner, M. F., Belew, R. K., Goodsell, D. S., and Olson, A. J. (2009). Autodock4 and autodocktools4: automated docking with selective receptor flexiblity. *J. Computational Chemistry*, 16:2785–2791.

Nazaroff, W. W. (2004). Indoor particle dynamics. *Indoor Air*, 14(7):175–183.

Nemmar, A., Hoylaerts, M. F., Hoet, P. H. M., Dinsdale, D., Smith, T., Xu, H., Vermylen, J., and Nemery, B. (2002). Ultrafine particles affect experimental thrombosis in an in vivo hamster model. *American Journal of Respiratory and Critical Care Medicine*, 166(7):998–1004.

Nenes, A., Pilinis, C., and Pandis, S. (1998). Isorropia: A new thermodynamic equilibrium model for multiphase multicomponent inorganic aerosols. *Aquat. Geochem.*, 4:123–152.

Nordenhall, C., Pourazar, J., Ledin, M., Levin, J., Sandtrom, T., and et al (2001). Diesel exhaust enhances airway responsiveness in asthmatic subjects. *Eur Respir J*, 17:909–915.

Oganesyan, V., Oganesyan, N., Terzyan, S., Qu, D., Dauter, Z., Esmon, N. L., and Esmon, C. T. (2002). The crystal structure of the endothelial protein c receptor and a bound phospholipid. *The Journal of Biological Chemistry*, 28:24851–24854.

Pai, P., Vijayaraghavan, K., and Seigneur, C. (2000). Particulate matter modeling in the los angeles basin using saqm-aero. *J. Air & Waste Manage. Assoc.*, 50:23–42.

Papaconstantinou, M. E., Carrell, C. J., Pineda, A. O., Bobofchak, K. M., Mathews, F. S., Flordellis, C. S., and Di Cera, E. (2005). Thrombin functions through its rgd sequence in a non-canonical conformation. *Journal Biological Chemistry*, 280:29393–29396.

Pathak, R. K., Louie, P. K., and Chan, C. K. (2004). Characteristics of aerosol acidity in hong kong. *Atmos. Environ.*, 38:2965–2974.

Penner, J., Charlson, R., Hales, J., Laulainen, N., Leifer, R., Novakov, T., andL.F. Radke, J. O., Schwartz, S., and Travis, L. (1994). Quantifying and minimizing uncertainty of climate forcing by anthropogenic aerosols,. *Bulletin of American Meteorological Society*, 75:375–400.

Penner, J., Eddleman, H., and Novakov, T. (1993). Towards the development of a global inventory for black carbon emissions. *Atmospheric Environment 27A*, 27A:1277–1295.

Pereira, P. J., Bergner, A., Macedo, R. S., Huber, R., Matschiner, G., Fritz, H., and Bode, W. (1998). Human beta-tryptase is a ring-like tetramer with active sites facing a central pore. *Nature*, 392:306–311.

Perrone, M. G., Larsen, B., Ferrero, L., Sangiorgi, G., De Gennaro, G., Udisti, R., Zangrando, R., Gambaro, A., and Bolzacchini, E. (2012). Sources of high pm2.5 concentrations in milan, northern italy: Molecular marker data and cmb modelling. *Sci. Total Environ.*, 414:343–355.

Pietropaoli, A., Frampton, M., Hyde, R., Morrow, P., Oberdorster, G., and et al (2004). Pulmonary function, diffusing capacity, and inflammation in healthy and asthmatic subjects exposed to ultrafine particles. *Inhal Toxicol*, 16(1):59–72.

Pilinis, C. and Seinfeld, J. H. (1987). Continued development of a general model for inorganic multicomponent atmospheric aerosols. *Atmos. Environ.*, 21:2453–2466.

Pope, C., Burnett, R., Thun, M., and et al (2002). Lung cancer, cardiopulmonary mortality, and long-term exposure to fine particulate air pollution. *JAMA*, 287(9):1132–1141.

Pope, C., Burnett, R., Thurston, G., Thun, M., Calle, E., and et al (2004). Cardiovascular mortality and long-term exposure to particulate air pollution. *Circulation*, 109:71–77.

Pope, C., Thun, M., Namboodiri, M., Dockery, D., Evans, J., Speizer, F., and Heath, C. (1995). Particulate air pollution as a predictor of mortality in a prospective study of u.s. adults. *Am J Respir Crit Care Med.*, 151:669–674.

Potukuchi, S. and Wexler, A. S. (1995). Identifying solid-aqueous-phase transitions atmospheric aerosol ii acidic solutions. *Atmospheric Environmental*, 29(22):3357–2264.

Quay, J., Reed, W., Samet, J., and Devlin, R. (1998). Air pollution particles induce il-6 gene expression in human airway epithelial cells via nf-kappab activation. *Am J Respir Cell Mol Biol*, 19(1):98–106.

Ramana, M., Ramanathan, V., Feng, Y., Yoon, S., Kim, S., Carmichael, G., and Schauer, J. (2010). Warming influenced by the ratio of black carbon to sulphate and the black-carbon source. *Nature Geoscience*, 3(8):542–545.

Ramanathan, V. and Feng, Y. (2009). Air pollution and greenhouse gases and climate change: Global and regional perspectives. *Atmospheric Environment*, 43(1):37–50.

Randriamiarisoa, H., Chazette, P., Couvert, P., and Sanak, J. (2006). Physics relative humidity impact on aerosol parameters in a paris suburban area. *Atmos. Chem. Phys*, 6:1389–1407.

Ridker, P., Rifai, N., Stampfer, M., and Hennekens, C. (2000). Plasma concentration of interleukin-6 and the risk of future myocardial infarction among apparently healthy men. *Circulation*, 101(15):1767–1772.

Riva, D., Magalhaes, C., Lopes, A., Lançcas, T., Mauad, T., and et al (2011). Low dose of fine particulate matter (pm2.5) can induce acute oxidative stress, inflammation and pulmonary impairment in healthy mice. *Inhal Toxicol*, 23(5):257–267.

Robock, A. (1991). Surface cooling due to forest fire smoke. *Journal of Geophysical Research*, 96:869–889.

Rohr, K. B., Selwood, T., Marquardt, U., Huber, R., Schechter, N. M., Bode, W., and Than, M. E. (2006). X-ray structures of free and leupeptin-complexed human alphai-tryptase mutants:indication for an alpha $-$ $>$ beta-tryptase transition. *Journal of Molecular Biology*, 17:195–209.

Rooij, J. V., Veeger, M., Bodelier-Bade, M., Scheepers, P., and Jongeneelen, F. (1994). Smoking and dietary intake of PAH as sources of interindividual variability in the baseline excretion of 1-hydroxypyrene in urine. *Int Arch Occup Environ Health.*, 66:55–65.

Rose, P. W., Bi, C., Bluhm, W. F., Christie, C. H., Dimitropoulos, D., Dutta, S., and Bourne, P. E. (2013). The rcsb protein data bank: New resources for research and education. *Nucleic Acids Research*, 41:475–482.

Sali, A. and Blundell, T. (1993). Comparative protein modeling by satisfaction of spatial restraints. *J Mol Biol*, 234:779–815.

Samet, J., Dominici, F., Curriero, F., Coursac, I., and Zeger, S. (2000). Fine particulate air pollution and mortality in 20 u.s. cities, 1987–1994. *N Engl J Med*, 343(24):1742–1749.

Samset, B., Myhre, G., Schulz, M., Balkanski, Y., Bauer, S., Berntsen, T., Bian, H., Bellouin, N., Diehl, T., Easter, R., Ghan, S., Iversen, T., Kinne, S., Kirkevag, A., Lamarque, J., Lin, G., Liu, X., Penner, J., Seland, Skeie, R., Stier, P., Takemura, T., Tsigaridis, K., Samset, K. Z. B., Myhre, G., Schulz, M., Balkanski, Y., Bauer, S., Berntsen, T., Bian, H., Bellouin, N., Diehl, T., Easter, R., Ghan, S., Iversen, T., Kinne, S., Kirkevag, A., Lamarque, J., Lin, G., Liu, X., Penner, J., Seland, Skeie, R., Stier, P., Takemura, T., Tsigaridis, K., and Zhang, K. (2013). Black carbon vertical profiles strongly affect its radiative forcing uncertainty. *Atmospheric Chemistry and Physics*, 13(5):2423–2434.

Saxena, P., Hudischewskyj, A., Seigneur, C., and Seinfeld, J. (1986). A comparative study of equilibrium approaches to the chemical characterization of secondary aerosols. *Atmos. Environ.*, 20:1471–1484.

Schicker, B., Kuhn, M., Fehr, R., Asmis, L., Karagiannidis, C., and Reinhart, W. (2009). Particulate matter inhalation during hay storing activity induces systemic inflammation and platelet aggregation. *Eur J Appl Physiol.*, 105(5):771–779.

Schwarz, J., Gao, R., Fahey, D., Thomson, D., Watts, L., Wilson, J., Reeves, J., Darbeheshti, M., Baumgardner, D., Kok, G., Chung, S., Schulz, M., Hendricks, J., Lauer, A., B.Karcher, Slowik, J., Rosenlof, K., Thompson, T., Langford, A., Loewenstein, M., and Aikin, K. (2006). Single-particle measurements of midlatitude black carbon and light-scattering aerosols from the boundary layer to the lower stratosphere. *Journal of Geophysical Research*, 111(D16).

Seinfeld, J. and Pandis, S. (1998). *Atmospheric chemistry and physics – From air pollution to climate change*. Wiley-Interscience edition.

Shehabi, A. (2009). *Energy Demands and Efficiency Strategies in Data Center Buildings*. PhD thesis, Civil and Environmental Engineering University of California, Berkeley.

Shehabi, A., Horvath, A., Tschudi, W., Gadgil, A. J., and Nazaroff, W. W. (2008). Particle concentrations in data centers. *Atmos. Environ.*, 42:5978–5990.

Shi, L. and Wu, J. (2009). Epigenetic regulation in mammalian preimplantation embryo development. *Reproductive Biology and Endocrinology*, 7.

Shields, H. C. and Weschler, C. J. (1998). Are indoor air pollutants threatening the reliability of your electronic equipment? *Heat/Piping/Air Cond.*, 70(5):46–54.

Shuichi, M. and Kollman, P. (1992). Settele: An analytical version of the shake and rattle algorithm for rigid water models. *J Comput Chem*, 8:952–962.

Silbajoris, R., Osornio-Vargas, A., Simmons, S., Reed, W., and et al, P. B. (2011). Ambient particulate matter induces il-8 expression through an alternative nf-b mechanism in human airway epithelial cells. *Environ Health Perspect*, 119:1379–1383.

Stafoggia, M., Faustini, A., Rognoni, M., Tessari, R., and et al, E. C. (2009). Air pollution and mortality in ten italian cities. *Epidemil Prev*, 33(6):65–76.

Steinvil, A., Kordova-Biezuner, L., Shapira, I., Berliner, S., and Rogowski, O. (2008). Short-term exposure to air pollution and inflammation-sensitive biomarkers. *Environ Res*, 106(1):51–61.

Stern, A., Boubel, R., and Turner, D. (1984). Fundamental of air pollution, 2nd edition,. *Academic Press, Inc.*

Stote R., K. M. (1995). Zinc binding in proteins and solution: a simple but accurate nonbonded representation. *Proteins*, 23:12–31.

Sullivan, J. H., Hubbard, R., Liu, S., Shepherd, K., Trenga, C., Koenig, J., Chandler, W., and Kaufman, J. D. (2007). A community study of the effect of particulate matter on blood measures of inflammation and thrombosis in an elderly population. *Environmental Health*.

Sun, Q., Wang, A., Jin, X., Natanzon, A., Duquaine, D., Brook, R., Aguinaldo, J., Fayad, Z., Fuster, V., Lippmann, M., Chen, L., and Rajagopalan, S. (2005). Long-term air pollution exposure and acceleration of atherosclerosis and vascular inflammation in an animal model. *JAMA. 2005 Dec 21;294(23):3003-10.*, 294(23):3003–3013.

(TC), A. T. C. (2009). Gaseous and particulate contamination guidelines for data centers. Technical report, ASHRAE.

(TC), A. T. C. (2011). Thermal guidelines for data processing environments – expanded data center classes and usage guidance. Technical report, ASHRAE.

Teilum, K., Olsen, J. G., and Kragelund, B. B. (2009). Functional aspects of protein flexibility. *Cellular Molecular Life Sciences*, 66:2231.2247.

Toussaint, S. and Gerlach, H. (2009). Activated protein c for sepsis. *The New England Journal of Medicine*, 361:2646–2652.

Tripathi, S., Srivastava, A., Dey, S., Satheesh, S., and Krishnamoorthy, K. (2007). The vertical profile of atmospheric heating rate of black carbon aerosols at kanpur in northern india. *Atmospheric Environment*, 41(32):6909–6915.

Trompetter, W. J., Grange, S. K., Davy, P. K., and Ancelet, T. (2013). Vertical and temporal variations of black carbon in new zealand urban areas during winter. *Atmospheric Environment*, 75:179–187.

Trott, O. and Olson, A. J. (2010). Autodock vina: Improving the speed and accuracy of docking with a new scoring function, efficient optimization and multithreading. *Journal of Computational Chemistry*, 31:455–461.

Van Der Spoel, D., Lindahl, E., Hess, B., Groenhof, G., Mark, A. E., and Berendsen, H. J. (2005). Gromacs: Fast, flexible, and free. *Journal of Computational Chemistry*, 16:1701–1718.

Van Gunsteren, W. F., Billeter, S. R., Eising, A. A., Huenenberger, P. H., Krueger, P., Mark, A. E., and Tironi, I. G. (1996). The gromos96 manual and user guide. *Simulation, biomolecular.*

Wallner, B. and Elofsson, A. (2003). Can correct protein models be identified? *Protein Sci.*, 12(5):1073–1086.

Wang, C., Schueler-Furman, O., and Baker, D. (2005). Improved side-chain modeling for protein-protein docking. *Protein Science*, 14:1328–1339.

Wang, H., Liu, Y., Huai, Q., Cai, J., Zoraghi, R., Francis, S., Corbin, J., Robinson, H., Xin, Z., Lin, G., and Ke, H. (2006). Multiple conformations of phosphodiesterase-5: implications for enzyme function and drug development. *J Biol Chem*, 281:21469–21479.

Wang, J., Wang, W., Kollman, P., and Case, D. (2001). Antechamber: an accessory software package for molecular mechanical calculations. *J Am Chem Soc*.

Weeks, J. I., Corbin, J., and Francis, S. (2009). Interactions between cyclic nucleotide phosphodiesterase 11 catalytic site and substrates or tadalafil and role of a critical gln-869 hydrogen bond. *J Pharmacol Exp Ther*, 331:133–141.

Wennberg, P., Wensley, F., Angelantonio, E. D., Johansson, L., Boman, K., Rumley, A., Lowe, G., Hallmans, G., Danesh, J., and Jansson, J. (2012). Haemostatic and inflammatory markers are independently associated with myocardial infarction in men and women. *Thromb Res*, 129(1):68–73.

Wexler, A. and Potukuchi, S. (1998). *Kinetics and thermodynamics of tropospheric aerosols, in Atmospheric Particles*. Wiley.

Wexler, A. and Seinfeld, J. (1991). Second-generation inorganic aerosol model. *Atmos. Environ.*, 25 (A):2731–2748.

Xiao, T., Takagi, J., Coller, B. S., Wang, J. H., and Springer, T. A. (2004). Structural basis for allostery in integrins and binding to fibrinogen-mimetic therapeutics. *Nature*, 432:59–67.

Xiong, J. P., Stehle, T., Diefenbach, B., Zhang, R., Dunker, R., Scott, D. L., and Arnaout, M. A. (2001). Crystal structure of the extracellular segment of integrin alpha vbeta3. *Science*, 294:339–345.

Xiong, J. P., Stehle, T., Zhang, R., Joachimiak, A., Frech, M., Goodman, S. L., and Arnaout, M. A. (2002). Crystal structure of the extracellular segment of integrin alpha vbeta3 in complex with an arg-gly-asp ligand. *Science*, 296:151–155.

Zarzycki, C. and Bond, T. (2010). How much can the vertical distribution of black carbon affect its global direct radiative forcing? *Geophysical Research Letters*, 37(20).

Zhang, Y. (2008). I-tasser server for protein 3d structure prediction. *BMC Bioinformatics*, 9(40).